RGS14$_{414}$-Mediated Activation of the 14-3-3ζ in Rodent Perirhinal Cortex Induces Dendritic Arborization, an Increase in Spine Number, Long-Lasting Memory Enhancement, and the Prevention of Memory Deficits

Irene Navarro-Lobato1,2,†, Mariam Masmudi-Martín1,2,‡, Manuel F. López-Aranda1,2,§, María E. Quiros-Ortega1,2, Marta Carretero-Rey1,2, María F. Garcia-Garrido1,2, , Carmen Gallardo-Martínez1,2, Elisa Martín-Montañez3, Celia Gaona-Romero1,2,GloriaDelgado1,2, Laura Torres-Garcia1,2, Javier Terrón-Melguizo1,2, Sinforiano Posadas1,2, Lourdes Rodríguez Muñoz1,2, Carlos Vivar Rios1,2, Jerome Zoidakis4, Antonia Vlahou4, Juan C. López5 and Zafar U. Khan1,2,6

1Laboratory of Neurobiology, CIMES, University of Malaga, Malaga 29010, Spain, 2Department of Medicine, Faculty of Medicine, University of Malaga, Malaga 29010, Spain, 3Department of Pharmacology, Faculty of Medicine, University of Malaga, Malaga 29010, Spain, 4Biotechnology Division, Biomedical Research Foundation of the Academy of Athens,Athens 11527,Greece, 5Animal Behavior and Neuroscience Lab., Department of Experimental Psychology, Faculty of Psychology, University of Seville, Seville 41018, Spain and 6CIBERNED, Institute of Health Carlos III, Madrid 28031, Spain

Address correspondence to Dr. Zafar U. Khan, Laboratorio de Neurobiología, Centro de Investigaciones Medico Sanitaria (CIMES), Calle Marqués de Beccaria, 3, Campus Teatinos s/n, Universidad de Málaga, Malaga 29010, Spain. Email: zkhan@uma.es.

†Current address: Donders Institute for Brain Cognition and Behaviour, Radboud University, Heyendaalseweg 135, Nijmegen 6525AJ, The Netherlands.

‡Current address: Brain Metastasis Group, National Cancer Research Centre (CNIO), Madrid 28029, Spain

§Current address: Department of Neurobiology, University of California-Los Angeles, Los Angeles, CA 90095, USA

|| Current address: Institute of Biomedical and Clinical Sciences, University of Exeter Medical School, Hatherly Laboratories, Exeter EX4 4PS, UK

Irene Navarro-Lobato and Mariam Masmudi-Martín contributed equally to this work.

Abstract

The remedy of memory deficits has been inadequate, as all potential candidates studied thus far have shown limited to no effects and a search for an effective strategy is ongoing. Here, we show that an expression of RGS14$_{414}$ in rat perirhinal cortex (PRh) produced long-lasting object recognition memory (ORM) enhancement and that this effect was mediated through the upregulation of 14-3-3ζ , which caused a boost in BDNF protein levels and increase in pyramidal neuron dendritic arborization and dendritic spine number. A knockdown of the 14-3-3ζ gene in rat or the deletion of the BDNF gene in

mice caused complete loss in ORM enhancement and increase in BDNF protein levels and neuronal plasticity, indicating that 14-3-3ζ-BDNF pathway-mediated structural plasticity is an essential step in $RGS14_{414}$-induced memory enhancement. We further observed that $RGS14_{414}$ treatment was able to prevent deficits in recognition, spatial, and temporal memory, which are types of memory that are particularly affected in patients with memory dysfunctions, in rodent models of aging and Alzheimer's disease. These results suggest that 14-3-3ζ-BDNF pathway might play an important role in the maintenance of the synaptic structures in PRh that support memory functions and that $RGS14_{414}$-mediated activation of this pathway could serve as a remedy to treat memory deficits.

Key words: 14-3-3ζ , BDNF, behavioral performance, cognitive dysfunction, episodic memory, memory circuit activation, memory deficits, memory enhancement, prevention of memory loss, regulator of G protein signaling.

Introduction

14-3-3ζ is a multifunctional protein that belongs to a conserved family of 14-3-3 proteins, and it is widely expressed in the mammalian brain (Aitken 2006). This protein family is one of the major constituents in the brain, accounting for almost 1% of total cytosolic proteins (Cornell and Toyo-Oka 2017). 14-3-3ζ interacts with many proteins and intercedes in several biological functions (Aitken 2006; Fan et al. 2019). This interaction usually involves the phosphorylation of the interacting protein (Aitken 2006). 14-3-3ζ has been implicated in aging and several neurological diseases, including Alzheimer's disease and schizophrenia (Umahara et al. 2012; Shimada et al. 2013; Fan et al. 2019). An in vitro study demonstrated that the phosphorylation of tau protein at Ser 214 by protein kinase A or protein kinase B augments its affinity for 14-3-3ζ binding up to 14-fold, and this interaction ultimately inhibits the formation of tau aggregates seen in Alzheimer's disease (Sadik, Tanaka, Kato, Yamamori, et al. 2009a; Sadik, Tanaka, Kato, Yanagi, et al. 2009b). 14-3-3ζ plays an essential role in regulating neurogenesis during cortical development (Toyo-oka et al. 2014) and is required for hippocampal long-term potentiation and associative learning and memory (Qiao et al. 2014). 14-3-3ζ is also considered as a possible genetic risk factor for neurodevelopmental disorders (Xu et al. 2015). Mice with a deletion in the 14-3-3ζ gene were found to display behavioral characteristics of schizophrenia such as hyperactivity and the disruption of sensorimotor gating (Cheah et al. 2012; Xu et al. 2015). The overexpression of 14-3-3ζ protected the neurons against the endoplasmic reticulum stress like response and vulnerability to excitotoxicity (Brennan et al. 2013). Moreover, 14-3-3ζ has been shown to play a central role in regulating multiple pathways that are responsible for cancer initiation and progression (Cornell and Toyo-Oka 2017; Gan et al. 2020). The first evidence that 14-3-3ζ is related to memory was found in *D. melanogaster*, where the leonardo gene, a homolog of vertebrate 14-3-3ζ , is abundantly expressed in mushroom body neurons. Mutant Drosophila that lacked the Leonardo gene showed a significant decrease in the

capacity for olfactory memory but not for olfactory sensory (Skoulakis and Davis 1996; Broadie et al. 1997; Skoulakis and Davis 1998). Similarly, mice lacking the 14-3-3ζ gene showed a decrease in their learning and recall abilities compared with their wild-type siblings (Cheah et al. 2012; Xu et al. 2015).A novel object recognition test revealed that these mutant mice had no preference between familiar objects and novel objects, and they exhibited a decreased discrimination index. A cross-maze escape task showed an increased escape latency and a reduced accuracy in arm choice in these mice. Moreover, a conditional rescue study of the behavioral phenotype in mutants of Drosophila further suggested an acute requirement of 14-3-3ζ in both learning and memory (Philip et al. 2001). Altogether, these studies in mice and Drosophila suggest that an increase in 14-3-3ζ could rescue animals from memory deficits. We previously showed that the expression of $RGS14_{414}$ protein in area V2 of the visual cortex and in the perirhinal cortex (PRh) of rodents induces memory enhancement and rescues memory deficits (López-Aranda et al. 2009; Masmudi-Martín et al. 2019), and now, we show that this $RGS14_{414}$-mediated memory enhancement is facilitated through an increase in 14-3-3ζ activity. An upregulation in 14-3-3ζ caused structural plasticity in dendrites of pyramidal neurons and long-lasting memory enhancement. Additionally, we found that this $RGS14_{414}$-mediated upregulation in 14-3-3ζ was sufficient for the prevention of object, spatial, and temporal memory, which are kinds of episodic memory that are primarily affected in patients or individuals with memory dysfunctions.

Materials and Methods

Lentivirus Preparation

The cDNA of human RGS14 (GenBank accession number AY987041) was cloned into the pLenti6/Ubc/V5-DEST Gateway vector (Thermo Fisher Scientific; catalog number V49910), and RGS14 lentivirus was produced according to the protocols of the ViraPower Lentiviral Expression System (Thermo Fisher Scientific). Vehicle lentivirus (vehicle) was prepared by vector alone.

Animals

In this study, we used rats, Alzheimer's disease mice, and brain derived neurotrophic factor (BDNF) knockout mice. In total 308 rats, 122 Alzheimer's disease mice, and 58 BDNF knockout mice were used in this study. All procedures were performed in accordance

with the guidelines of the Institutional Animal Care and Use Committee (IACUC) of the University of Malaga. Protocols (CEUMA 32-2016-A and 7-2017-A) for performing the experiments were approved by the IACUC of University of Malaga. Both rats and mice were housed in a temperature-regulated (20±2 ◦C) room under a 12-h light/dark cycle. Drinking water and food were available ad libitum except when indicated. The animals were acclimatized to the room for at least 1 week before starting the experiments, which took place during the light phase. All possible measures are taken to maintain the good health and well-being of animals. Both departmental and veterinary staffs closely monitor

animals and test routinely for the infection and diseases. Anesthetics were used in accordance with the guidelines of the IACUC of the University of Malaga to minimize suffering of animals during the surgery as well as the sacrifice.

Rats

Wistar Han rats (research resource identifier (RRID), RGD_2308816) obtained from Charles River were used for this study. One to two rats were housed per cage. Rats of 3 months of age were used for the experiments that are presented in Figures 2–4, and rats of 6 and 12 months of age were used for the experiments that are presented in Figure 5. In total, 308 rats were used in this study where 40 rats were for untreated group, 117 rats were for vehicle-treated group, 119 rats were for $RGS14_{414}$-treated group, 16 rats for $RGS14_{414}$ +control shRNA group, and 16 rats for RGS14+14-3-3ζ shRNA group. Two rats of each untreated, vehicle and RGS14 groups presented in Figure 5*A*,*B* died during the course of experimentation between the age of 19 and 24 months and they were not replaced.

Transgenic Mice with Alzheimer's Disease (AD Mice)

The transgenic hAPPSwInd (J20) mice used in this study were from the Jackson Laboratory (stock number 006293). These mice express a mutant form of human APP bearing both Swedish (K670N/M671L) and Indiana (V717F) mutations associated with familial Alzheimer's disease (Mucke et al. 2000). Mutated APP expression is directed to neurons under the control of the human platelet-derived growth factor β chain (PDGFB) promoter. These mice were inbred on the C57BL/6J genetic background. Aβ deposition has been observed to appear at the age of 6 months. These mice show synaptic and cognitive impairments, among other characteristics of Alzheimer's disease, and have been widely used for cognitive studies (Palop et al. 2003; Chin et al. 2005). Four to five mice were housed in each cage. AD mice and wild-type C57BL/6J mice of 2.5 months of age were used for the experiments shown in Figure 6. In total, 122 mice were used in this study where 31 mice were for wild-type group, 30mice were for AD mice group, 29 AD mice were for vehicle treatment group, and 32 AD mice for $RGS14_{414}$ treatment.

BDNF Knockout Mice

BDNF knockout mice were from the Jackson Laboratory (stock number 002266) (Ernfors et al. 1994). In our studies, 3-month-old mice heterozygous for the BDNF mutation (BDNF+/−) were used for the experiments shown in Figure 4*C*,*D*. Wild-type littermate mice were used as controls. In total, 58 BDNF knockout mice were used in this study where 10 mice were for wild-type group, 16 wild-type mice were for vehicle treatment group, 16wild-type mice were for $RGS14_{414}$ treatment group, and 16 BDNF+/− mice were for $RGS14_{414}$ treatment group.

Lentivirus Delivery

Rats and mice were anesthetized with the sevoflurane system (induction at 5% sevoflurane +1 L/min O2 and maintenance at 2% sevoflurane +0.4 L/min O2) and placed

in a stereotaxic frame according to the coordinates obtained from Steriotaxic Coordinates of the Rat Brain by Paxinos and Watson (fourth edition) (Paxinos and Watson 1998) and The Mouse Brain by Paxinos and Franklin (second edition) (Paxinos and Franklin 2001). The coordinates of the injection site in the perirhinal cortex were AP −4.52, ML ±6.7, and DV −4.75 (rats) and AP −1.9, ML±3.9, and DV −2.20 (mice). A total volume of 2 μL of $RGS14_{414}$ lentivirus from a stock titer of 2.3×107 TU/mL was injected bilaterally (1 μL in each hemisphere) through a 30-gauge stainless steel internal cannula in both rats and mice. During surgery, animal body temperature was maintained with an electric blanket. After surgery, animals were treated daily for 5 days with local antibiotic (as Dermocan manufactured by Fatro) application on the incision and 150-μL intraperitoneal injection of Meloxicam analgesic (as Metacam 5 mg/mL manufactured by Boehringer Ingelheim) and then, they were left until the experiments started. Behavioral tests were generally performed 20 days after injection. However, some tests were performed between 10 and 180 days after injection, as shown in Figures 2*B*,*D*,*E* and 4*E*; 6–12 months after injection, as shown in Figure 5; and 2.5–7.5 months after injection, as shown in Figure 6. To evaluate the surface area affected by $RGS14_{414}$ lentivirus injection in the PRh, the brains of rats from Figure 1*A* were processed after behavioral studies. Similar to earlier studies (Masmudi-Martín et al. 2019), an analysis of coronal brain sections indicated that the expression of $RGS14_{414}$ protein was limited to the PRh area (drawings in red color in Supplementary Fig. 1).

Brain Extraction

Before proceeding for brain extraction, animals were deeply anesthetized by administering intraperitoneally 75-mg/kg ketamine (as Imalgene 1000 manufactured by Merial Laboratorios) and 1 mg/kg (rats) or 0.5 mg/kg (mice) of medetomidine (as Domtor manufactured by Pfizer). After deep anesthesia, animals were decapitated by guillotine and their brains were dissected out and carefully PRh area was extracted with a 4-mm punch (DH Material Médico, catalog number 94158BP-40F).

Object Recognition Memory (ORM) Test in Rats

The ORM test was performed as described previously (Ennaceur and Delacour 1988; López-Aranda et al. 2009; Masmudi-Martín et al. 2019). Prior to the test, rats were handled for 8 min daily for five consecutive days, and the next 2 days, they were habituated in an open field (100×100×50 cm) for 12 min. On the day of the experiment and in the object exposure session, the rats were placed in the same open field with two identical objects and were allowed to freely explore the area for 3min. In general, after a delay of 24 h, the animals were tested for ORM status with one previously presented object (familiar) and a novel object; however, the delay period was adjusted from 30 min to 4 weeks, as shown in Figure 1*A*. The location of the novel object was changed arbitrarily between the left and right sides. The open field was cleaned after each session. Objects shown previously were never presented to the same animal in any future sessions. The sessions were video recorded. The exploration time was calculated from the video by two independent persons. Exploration time was defined as only when the animal was

touching the object with its nose. Standing using the object as a support was not counted. Animals with more than 20 days of rest from the last ORM test were again handled and habituated prior to the next ORM test. The average total exploration time of the objects (familiar+novel) during the ORM test session of vehicle and $RGS14_{414}$ lentivirus-treated animals was 28.25 ±2.03 and 29.67±2.39 s, respectively. The discrimination index (DI) presented in Figures 1*A*, 2*B*, 3*D*, and 5*A* was calculated by dividing the time spent exploring the novel object by the total exploration time (familiar object+novel object).A DI equal to or less than 0.5 indicates that the animals were unable to retain object information in memory because they explored both familiar and novel objects for equal times (familiar object 50% and novel object 50%), whereas a DI above 0.66 indicates that the animals were able to successfully retain information about the object in memory because they spent more than 66% of the total time exploring novel objects and less than 34% of the time exploring familiar objects. Unfilled circles within each bar of the figures reflect the DI values of each of the animals used in that experiment.

Dendritic Arborization

Rat and mouse brains were processed for Golgi-Cox staining using a Rapid Golgi Stain kit (FD Neurotechnologies; catalog number PK401) following the protocol from the manufacturer. All procedures were performed protected from light. A 180-μm section was prepared with a cryostat, and after staining, the sections were mounted with Permount mounting medium (Thermo Fisher Scientific; catalog number SP15-100). Pyramidal neuronal branching was analyzed in the area of injection under a DM IRE2 microscope (Leica Microsystems) using Leica MM AF software, version 1.6.0 (Leica Microsystems). A total of 34–56 pyramidal neurons were studied in the vehicle lentivirus-treated group, and 35–79 neurons were studied in the RGS lentivirus-treated group. The number of branches of apical dendrites in pyramidal neurons was determined. Spines were counted from the apical dendrites of pyramidal neurons according to their physical appearance into the thin, mushroom, and stubby groups, as described previously (Morrison and Baxter 2012). However, there was no difference between vehicle and RGS-treated animals in any of the groups, and therefore, they were combined. Results of the dendritic branching and spine counts are presented in Figures 2C,*D*,*E*, 3*C*, and 4*C*.

Proteomics

Four-millimeter rat brain punches from the injected area were obtained at 5, 10, and 20 days after RGS or vehicle treatment and were homogenized in solubilization buffer (7 M urea, 2 M thiourea, 4% CHAPS, 1% dithioerythritol). Homogenized samples were centrifuged at 13 000 rpm (Beckman CS-15R, rotor F2402H) for 15 min at 4 ◦C, and the supernatant was collected. Proteins from the supernatant samples were separated by two-dimensional electrophoresis (2-DE). In the first dimension of electrophoresis, proteins were separated horizontally by an isoelectric force using an immobilized pH gradient and electric current. In the second dimension of electrophoresis, the protein bands after the first dimension of electrophoresis were further separated by SDS-PAGE using 12% polyacrylamide mini gels, and then, the gels were stained with 0.12% Brilliant Blue G-

Colloidal dye solution. Stained gels were scanned with a calibrated imaging densitometer (Model GS-800 of Bio-Rad), and automated spot density matching was performed for differential expression pattern analysis between vehicle- and RGS14-treated animals. For the identification of proteins, excised gel spots were processed for tryptic digestion and peptide extraction and were further subjected to MALDI TOF-TOF mass spectrometry. The results obtained from the mass spectrometer were compared with available database systems to identify the protein of a selected gel spot. Results of 2-DE gels and spot density analysis corresponding to 14-3-3ζ protein are in Figure 3*A.i*,*A.ii*.

Western Blots

Blots were performed as described previously (Khan et al. 1993; Masmudi-Martín et al. 2019). A 4-mm punch was extracted from the injected area of the rat brain and homogenized in 100 mM Tris–HCl buffer, pH 8.0, with 1% protease inhibitor cocktail (Sigma-Aldrich; catalog number P8340) and 1% phosphatase inhibitor cocktail (Sigma-Aldrich; catalog number P2850). For isolation of the nuclear fraction, the homogenate was centrifuged at 1000*g* for 10 min at 4 ◦C, and the nuclear pellet was suspended in 10mMPBS buffer, pH 7.4. After treatment with SDS buffer, whole-homogenate proteins or nuclear proteins were separated on 4–20% Mini-Protein TGX Stain-Free Gels (Bio-Rad; catalog number 4568095) and transblotted onto PVDF membranes of the Trans-Blot Turbo Transfer Packs kit from Bio-Rad (catalog number 1704157). Membranes containing proteins were incubated with rabbit anti-14-3-3ζ (1:4000 dilution; Santa Cruz Biotechnology; catalog number sc1019), mouse anti-RACK1 (1:500 dilution; Santa Cruz Biotechnology; catalog number sc17754), or goat anti-BDNF (pro) (1:1000 dilution; Santa Cruz Biotechnology; catalog number sc33904), followed by incubation with goat anti-rabbit IgG-HRP (1:20 000 dilution; Sigma-Aldrich), rabbit anti-mouse IgG-HRP (1:20 000 dilution; Sigma-Aldrich), or donkey anti-goat IgG-HRP (1:20 000 dilution; Life Technologies). Bands were visualized by using Immobilon Western Chemiluminescent HRP Substrate (Millipore; WBKLS0500), and images were acquired with a ChemiDocMP Imaging System and ImageLab Software (both from Bio-Rad). Densitometry analysis of the immunoreactive bands was performed with ImageLab Software, and all values were normalized to the total protein of the corresponding lane. A single immunoreactive band was identified at 28 kDa for 14-3-3ζ protein, at 35 kDa for RACK1, and at 32 kDa for BDNF (pro) protein (Supplementary Fig. 2). Results of optical density analysis are presented in Figures 3*B.i*,*B.ii* and 4*A.i*,*A.ii*,*B.ii*,*B.iii*,*E*. In Figure 3*B.i*, 2.5- and 5-μg total protein was loaded from each sample, and in Figure 4*A.i*,*B.ii*,*E*, 5- and 10-μg total protein was loaded. Unfilled circles within each bar of the figures reflect the number of experiments where two–three experiments were done from each of the two sets of brain homogenate prepared from a pool of four animal brain in each set. Each unfilled circle in bars represents the average of the values from the lanes of 2.5- and 5-μg protein or 5- and 10-μg protein.

Knockdown of 14-3-3ζ Gene in Rats

Small hairpin RNA (shRNA) adeno-associated virus (AAV) particles of the rats 14-3-3ζ gene (GenBank accession NM_013011.3) were purchased from GeneCopoeia (catalog

number AA10-RSE049324-AVE001-200). Control shRNA AAV particles were also from GeneCopoeia (catalog number AC202). Rats were injected stereotaxically with a total of 2 μL containing 1$\times$1010 GC AAV particles of shRNA of the 14-3-3ζ gene or control shRNA bilaterally (1 μL in each hemisphere) in the perirhinal cortex at coordinates similar to those described above for lentivirus delivery. Seven days after the injection, both groups of shRNA rats were injected with the lentivirus of $RGS14_{414}$ gene as in lentivirus delivery. These rats were then used for experiments after 27 days of the shRNA injection, which is 20 days after $RGS14_{414}$ gene treatment. In initial experiments to determine the efficacy of 14-3-3ζ gene knockdown with western blot method, we observed that a treatment with the shRNA of 14-3-3ζ in normal rats reduced 14-3-3ζ protein expression to 24.37$\pm$2.49% (n=4; two experiments from each of the two sets of brain homogenate prepared from a pool of four animal brain in each set) and in RGS-PRh rats reduced 14-3-3ζ protein expression to 27.02$\pm$2.20% (n=6; three experiments from each of the two sets) (Supplementary Fig. 3). Results of the experiments with knockdown of 14-3-3ζ are shown in Figure 3*C,D*.

Quantitative RT-PCR (qRT-PCR)

qRT-PCR was performed similar to as described earlier (Masmudi-Martín et al. 2019). A 4-mm punch was extracted from the injected area of the rat brain. They were then processed for RNA extraction with the RNeasy Tissue Mini kit (Qiagen; catalog number 74124). cDNAs of purified RNA samples were prepared with the High Capacity RNA-to-cDNA kit (Applied Biosystems; catalog number 4387406). To determine BDNF mRNA levels, quantitative RT-PCR was performed. A specific forward primer AAGCAATATTTCTACGAGACCAAGTG and reverse primer TACGATTGGGTAGTTCGGCATT of the BDNF gene (GenBank accession NM_001270630.1) were designed. After primer optimization and standard curve analysis, qRT-PCR reaction was performed in a thermocycler 7500 Real-Time PCR System (Applied Biosystems) using the Power SYBR Green PCR Master Mix kit (Applied Biosystems; catalog number 4367659). For quality control of the qRT-PCR reaction of each sample, five sequential cDNA concentrations consisting of 40, 80, 160, 320, and 640 ng were included, where Ct values of each following concentration were expected to be 1 and mRNA levels twice high. Ribosomal protein L19 (Rpl19) was used as a housekeeping gene, and the values of the BDNF gene were normalized to this gene. Results of BDNF mRNA levels in Figure 4*B.i* are average of the five concentrations.

ORM Test in BDNF +/− Mice

For this study, we have used heterozygous BDNF mutant mice as previously (Masmudi-Martín et al. 2019). The ORM test in mice was very similar to that in rats, except in the exploration session, the mice were exposed to two identical objects for 5min. The size of the open field was smaller (50$\times$35$\times$50 cm). In the ORM test session, the retention of object information in memory was evaluated after a delay of 24 h. The DI values shown in Figure 4*D* were calculated similar to those in rats. A DI above 0.66 indicates that the animals were able to retain information about the objects in memory. The average total

time exploring objects (familiar+novel) during the ORM test session of vehicleand $RGS14_{414}$ lentivirus-treated BDNF+/− mice was 22.28±3.51 s and 20.93±2.47 s, respectively.

We observed that the performance on ORM test of heterozygous mice was similar to that of wild-type mice on the ORM task at 45 min and 24 h. Similar to rats (Fig. 1*A*), both wild-type and BDNF+/− mice were able to recall object information from memory after 45 min (wild-type, 0.702±0.024; BDNF+/−, 0.698±0.022); however, they were unable to recall object information after 24 h (wild-type, 0.498±0.019; BDNF+/−, 0.501±0.020). Thus, heterozygous BDNF mutant mice displayed sufficient memory capacity to discriminate between novel and familiar objects during the performance on the ORM task in our experimental conditions.

Spatial Memory Test

Spatial memory was tested according to the open field Morris water maze (MWM) procedure, as described previously, with some modifications (Morris 1984; Masmudi-Martín et al. 2019). Briefly, an escape platform was hidden 2 cm below the water surface in a fixed location in one of the four quadrants of the water maze. During 4 days of training, the animals were required to locate the submerged invisible platform by using distal extramaze cues. The animals were subjected to four trials of 60 s each day. On the day 4 of training, the time to reach the hidden platform (latency), and on the day 5, exploration time spent in the quadrant area where platform was located on day 4 were measured using a computerized tracking system (EthoVision XT; Noldus Information Technology). Latency was calculated from day 4 of training and the results are presented in Figures 5*B* and 6*B*.

Temporal Memory Test

The conditioned taste aversion (CTA) paradigm was used for this test (Masmudi-Martín et al. 2019). Water-deprived animals were given water daily in the morning (8.00 h) and saccharine solution (0.4 g/L) at night (18.00 h) for 10 min. On the third morning, the animals were given saccharine solution instead of water, and immediately after their drinking session, they received an intraperitoneal injection of lithium chloride (0.1 M) to induce a weak CTA. At night on the day of conditioning, the animals were given water. The day after conditioning, the animals were given water in the morning and at night. Afterward, during five consecutive days of extinction, the animals were allowed to drink water in the morning and saccharine solution at night. In the morning on the day of the test, a time of the day when conditioning was done, the animals were exposed to saccharine solution. Apart from saccharine solution, which was used for studies at 6 months, different taste solutions, including sodium chloride saline solution (0.16 M), monosodium glutamate solution (0.1 M), or acetic acid solution (1.2%), were used at 12, 18, and 24months. The daily taste solution intake was recorded throughout the experiment, and the percentage of solution intake was analyzed. The results of the consumption of sucrose or other taste solutions in the morning of test day are shown in Figures 5*C* and 6*C*.

ORM Test in AD Mice

The ORM test in AD mice was very similar to that in BDNF mice, with some exceptions (Escribano et al. 2009; Masmudi-Martín et al. 2019). In the exploration session, the mice were exposed twice for 10 min each to two identical objects with 10 min between each exposure. The calculation of DI values shown in Figure 6*A* was similar to that in rats.

Statistics

The results were plotted and statistical significance was evaluated using Prism 8. The data used to construct Figures 1–6 passed the normality test done by the Shapiro–Wilk normality test, and they showed *P* values ranged from 0.083 to 0.987. The equality of group variances was tested by the Brown–Forsythe test, and the *P* values ranged from 0.106 to 0.997. Two-group comparisons were analyzed using two-tailed unpaired *t* tests. More than two group comparisons with single variables were analyzed using one-way ANOVA with Tukey's post hoc test. For multiple group comparisons with more than one variable, two-way ANOVA with the Sidak's post hoc test was used. All data in the figures are presented as the mean ± SEM values.

Results

$RGS14_{414}$ Gene Treatment in PRh Produced Long-Lasting ORM Enhancer Capacity

The perirhinal cortex (PRh) is a brain area that plays a central role in processing object recognition memory (ORM) (Brown and Aggleton 2001; Murray and Richmond 2001) and serves as one of the main memory hubs, where various kinds of memory converge (Masmudi-Martín et al. 2019). We showed that overexpression of $RGS14_{414}$ protein in this brain area induces ORM enhancement (Masmudi-Martín et al. 2019). RGS rats were able to hold object information in memory after a delay of 24 h; however, untreated normal rats could retain only the same object information for 45 min. Here, we have studied whether $RGS14_{414}$ protein overexpression in the PRh can cause long-lasting change in this memory or not. A lentivirus containing the $RGS14_{414}$ gene was delivered into the PRh of Wistar Han rats to induce expression of the $RGS14_{414}$ protein, and the memory status of these animals was evaluated 20 days after treatment by their performance on the ORM task, which is considered a hallmark test of recognition memory (Winters et al. 2008). We observed that when normal untreated 3-month-old rats were exposed to an object for 3 min, they were able to retain information about the object in memory after a delay of 30 or 45 min but not after a delay of 24 h (Fig. 1*A*; one-way ANOVA, $F(3, 44)=51.67$; 30 and 45 min versus 24 h, Tukey's post hoc test, $P<0.0001$). However, rats treated with the $RGS14_{414}$ gene in the PRh (RGS-PRh rats) were able to retain the same object information in memory after a delay of 24 h, 1week, or even 4weeks (Fig. 1*A*; two-way ANOVA, $F(1, 22)=151.6$; vehicle versus RGS14 at 24 h, 1 week, or 4 weeks, Sidak's post hoc test, $P<0.0001$). Animals treated with lentivirus vehicle (vehicle), saline solution, or lentivirus containing RGS12, a protein that belongs to the same family as $RGS14_{414}$, did not induce the rats to retain this object information in memory (Supplementary Fig. 4), and the performance of these rats in the test was similar

to the performance of untreated rats (24 h in Fig. 1*A*). These results suggest that $RGS14_{414}$ gene treatment induced ORM enhancement to the extent that it led to the transformation of short-term memory from 45 min into long-lasting long-term memory, which could be recalled after several weeks.

Considering the robust ORM enhancement in RGS-PRh animals, we next explored how long this ORM enhancer effect of $RGS14_{414}$ persists after a treatment in PRh. Rats treated with the $RGS14_{414}$ gene were tested for their ORM status 10–180 days after treatment. On the day of the test, RGS-PRh rats were exposed to an object, and their ORM levels were evaluated after a delay of 24 h. We found that RGS14-mediated ORM enhancement was similar to as in Figure 1*A* at 20 days after the treatment (Fig. 1*B*; two-way ANOVA, $F(1, 18) = 192.9$; vehicle versus RGS14 at 20 days; Sidak's multiple comparisons test, $P<0.0001$), and this memory enhancer effect of $RGS14_{414}$ was preserved 30 ($P<0.0001$), 90 ($P<0.0001$), and 180 ($P<0.0001$) days after the treatment. In contrast, the ORM enhancement was not observed at 10 days after the treatment. Together, these results demonstrate that the effect of $RGS14_{414}$ treatment on ORM did not surface immediately; instead, this memory-related behavior in RGS-PRh rats took 20 days to express, and once this ORM enhancer effect appeared in these rats, it endured for a long time.

$RGS14_{414}$ Gene Treatment in the PRh Induced Dendritic Arborization and Caused a Boost in Spine Number

We hypothesized that this long-lasting ORM enhancer effect of $RGS14_{414}$ might be due to permanent changes in neuronal structures, such as dendritic remodeling, a type of structural plasticity that is thought to be intimately related to synaptic plasticity and learning and memory (Lamprecht and LeDoux 2004). Therefore, rat brains obtained 20 and 60 days after $RGS14_{414}$ gene treatment were subjected to Golgi–Cox silver staining, and a Sholl analysis and an analysis of proliferation in dendritic branching and apical and basal dendritic synaptic density of pyramidal neurons were performed. Both the images of Golgistained neurons and the drawing of pyramidal neurons from RGS-PRh rat brains show robust dendritic arborization (neuronal image in Fig. 2*A* and neuronal depiction in Fig. 2*B*). $RGS14_{414}$ treatment in the rat brain caused an increase in dendritic neuronal arborization (Fig. 2*C* Sholl analysis; two-tailed unpaired *t* test, $P<0.0001$) and an almost 2-fold increase in dendritic branching of pyramidal neurons (Fig. 2*D*; two-way ANOVA, $F(1, 20)=127.2$; vehicle versus RGS14 at 20 and 60 days, Sidak's post hoc test, $P<0.0001$). However, this increase in dendritic branching reached a maximum level 20 days after treatment because there was no difference in dendritic branching between 20 and 60 days after treatment. Furthermore, consistent with this observation, the total number of apical dendritic spines (Fig. 2*E*; two-way ANOVA, $F(1, 20)=384.2$; vehicle versus RGS14 at 20 and 60 days, Sidak's post hoc test, $P<0.0001$) and of basal dendritic spines (Fig. 2*F*; two-way ANOVA, $F(1, 20)=228.9$; vehicle versus RGS14 at 20 and 60 days, Sidak's post hoc test, $P<0.0001$) was considerably higher in RGS-PRh rats than in vehicle-treated animals. However, similar to dendritic branching, no difference in spine number was observed between 20 and 60 days after treatment. These results suggest that the robust structural plasticity seen in both dendrites and spines in RGS-PRh rats occurred

in 20 days of the treatment, after which the ORM enhancer effect surfaced in these animals.

14-3-3ζ Mediates Dendritic Arborization and ORM Enhancement in RGS-PRh Animals

To shed light on the underlying mechanism of RGS-mediated memory enhancement, we set out to identify proteins that respond to $RGS14_{414}$ gene treatment. Therefore, a differential protein expression analysis was performed with the use of proteomics in rats after 5, 10, and 20 days of $RGS14_{414}$ gene treatment. The proteins of brain extracts were separated by two-dimensional electrophoresis (2-DE), and the optical density (O.D.) values of protein spots in blue silver stained gel were obtained by densitometry analysis. Each spot was then excised and subjected to MALDI-TOF-TOF mass spectrometry for protein identification. We detected a protein named 14-3-3ζ that responded strongly to $RGS14_{414}$ treatment. An increase in 14-3-3ζ protein expression was evident in the 2-DE gel image (Fig. 3*A.i*; protein spot in the white circle in the gel images of vehicle and RGS14), and the normalized O.D. analysis of the 14-3-3ζ protein spot in the 2-DE gel showed a progressive increase in the expression of this protein after 10 and 20 days of treatment (Fig. 3*A.ii*; two-way ANOVA, $F(1, 6)=296.5$; vehicle versus RGS14 at 10 and 20 days, Sidak's post hoc test, $P<0.0001$). This increase in 14-3-3ζ protein level observed in the 2-DE gel protein spot analysis was further confirmed by western blotting. The extracted brains of rats 20 days after $RGS14_{414}$ gene treatment were processed for western blot analysis. The plot of the O.D. values of the protein bands from the western blot in Figure 3*B.i* revealed an increase in 14-3-3ζ protein levels in both lanes where 2.5- and 5-μg total protein was loaded (Fig. 3*B.ii*; two-way ANOVA, $F(1, 6)=245$; vehicle versus RGS14 at 2.5 and 5 μg, Sidak's post hoc test, $P<0.0001$).¡.

A coincidence of elevated 14-3-3ζ protein expression with the emergence of the ORM enhancer effect in RGS-PRh animals led us to hypothesize that this protein might be implicated in this process. Therefore, to evaluate the extent of 14-3-3ζ involvement in RGS14-mediated dendritic arborization and ORM enhancement, RGS-PRh rats were subjected to treatment with shRNA of 14-3-3ζ with the goal of curbing the expression of 14-3-3ζ protein in PRh. This shRNA treatment reduced the expression of 14-3-3ζ protein to 27.02±2.20% in rats (Supplementary Fig. 3). RGS-PRh rats without treatment with shRNA of 14-3-3ζ showed an increase in dendritic branching in pyramidal neurons (Fig. 3*C*; one-way ANOVA, $F(3, 20)=37.64$; vehicle versus RGS14, Tukey's post hoc test, $P < 0.0001$).However, when the same RGS-PRh rats were treated with shRNA of 14-3-3ζ , the effect on dendritic proliferation disappeared, and these rats showed dendritic branching in pyramidal neurons similar to those of vehicle- or 14-3-3ζ shRNA-treated control rats (Fig. 3*C*; one-way ANOVA, $F(3, 20)=37.64$; RGS14+shRNA control versus RGS14+14-3-3ζ shRNA, Tukey's post hoc test, $P < 0.0001$). In addition to dendritic proliferation, we further studied the effect of 14-3-3ζ shRNA treatment on ORM enhancement in RGS-PRh rats. Similar to above studies, rats treated with the $RGS14_{414}$ gene showed ORM enhancement (Fig. 3*D*; one-way ANOVA, $F(3, 36)=19.35$; vehicle versus RGS14, Tukey's post hoc test, $P < 0.0001$); however, the same RGS-PRh rats treated with 14-3-3ζ shRNA exhibited abrogated memory-enhancing effect of $RGS14_{414}$

(Fig. 3*D*; one-way ANOVA, $F(3, 36)=19.35$; RGS14+shRNA control versus RGS14+14-3-3ζ shRNA, Tukey's post hoc test, $P < 0.0001$). In contrast to rats subjected to $RGS14_{414}$ gene treatment, normal rats treated with either vehicle or shRNA of 14-3-3ζ exhibited no change in ORM. The complete loss of RGS-mediated neuronal arborization and ORM enhancement after 14-3-3ζ knockdown suggests that $RGS14_{414}$ exerts its function primarily through the regulation of 14-3-3ζ.

The 14-3-3ζ-BDNF Pathway Facilitates RGS14-Mediated Structural Plasticity and Memory Enhancement

The 14-3-3ζ protein forms a complex with receptor for activated C kinase 1 (RACK1) and is then transported to the nucleus, where it binds to exon IV of BDNF and promotes transcription of the BDNF gene (Neasta et al. 2012). Therefore, high 14-3-3ζ protein levels in RGS-PRh animals might facilitate the transport of RACK1 to the nucleus and increase BDNF transcription. This hypothesis dictates that there should be higher levels of RACK1 and 14-3-3ζ proteins in the nuclei of RGS-PRh animals. Hence, we next tested the level of both proteins in the nuclei of rats treated with the $RGS14_{414}$ gene. Extracted brains of RGS-PRh rats were processed for preparation of the nuclear fraction, and then, the nuclear fractions were used for western blotting. The plot of the O.D. values of the protein bands from the western blot in Figure 4*A.i* showed increases of 40.01±2.28% in 14-3-3ζ protein levels (Fig. 4*A.ii*; two-way ANOVA, $F(1, 14)=612.5$; vehicle versus RGS14, Sidak's post hoc test, $P<0.0001$) and 37.83±2.44% in RACK1 protein levels (Fig. 4*A.ii*; two-way ANOVA, $F(1, 14)=612.5$; vehicle versus RGS14, Sidak's post hoc test, $P<0.0001$). The similar level of increase in both RACK1 and 14-3-3ζ proteins suggests that 14-3-3ζ might facilitate the increase in BDNF in RGS14-treated animals. Therefore, we next explored the mRNA and protein levels of BDNF in RGS-PRh rats. We first evaluated them RNA levels of BDNF and then examined their protein levels by western blotting. qRT-PCR analysis revealed that the mRNA levels of BDNF in RGS-treated animals were 118±6.80% higher than those in vehicle-treated control animals (Fig. 4*B.i*; vehicle versus RGS14; two-tailed unpaired *t* test, $P<0.0001$). These results indicate that $RGS14_{414}$ treatment exerts a strong effect on BDNF mRNA levels through the regulation of 14-3-3ζ protein levels. We next examined the effect of $RGS14_{414}$ treatment on BDNF protein levels. The plot of the O.D. values of the protein bands from the western blot in Figure 4*B.ii* showed a 71.67±3.71% increase in BDNF protein levels (Fig. 4*B.iii*; vehicle versus RGS14; two-tailed unpaired *t* test, $P<0.0001$). This marked increase in BDNF protein expression in RGS-PRh animals indicates that 14- 3-3ζ mediates the effect of $RGS14_{414}$ through regulation of BDNF signaling.

Permanent structural plasticity that causes a long-term change in memory functions, such as that observed in $RGS14_{414}$-treated rats, has often been associated with BDNF (McAllister et al. 1999; Waterhouse and Xu 2009). Therefore, to further evaluate BDNF involvement in RGS14-mediated neuronal arborization and ORM enhancement, heterozygous mutant mice of BDNF (BDNF+/−) were included in this study. Similar to rats, wild-type mice subjected to $RGS14_{414}$ gene treatment in the PRh showed an increase in dendritic branching in pyramidal neurons (Fig. 4*C*; one-way ANOVA, $F(2, 15)=23.27$;

wild-type+vehicle versus wild-type+RGS14, Tukey's post hoc test, $P < 0.0001$). However, when the same treatment was performed in BDNF+/− mice, the effect on dendritic proliferation disappeared, and the BDNF+/− mice showed dendritic branching in pyramidal neurons similar to that in wild-type vehicle-treated mice (Fig. 4*C*; one-way ANOVA, $F(2, 15)=23.27$; wild-type+RGS14 versus BDNF+/− +RGS14, Tukey's post hoc test, $P=0.0001$).

In addition to neuronal proliferation, we further studied the effect of $RGS14_{414}$ gene treatment on ORM enhancement in BDNF+/− mice. Treatment of wild-type mice with the $RGS14_{414}$ gene led to ORM enhancement similar to that in rats (Fig. 4*D*; one-way ANOVA, $F(3, 36)=6.995$; wild-type or wild-type+vehicle versus wild-type+RGS14, Tukey's post hoc test, $P<0.005$); however, the same treatment in BDNF+/− mice abrogated the memory-enhancing effect of $RGS14_{414}$ (Fig. 4*D*; one-way ANOVA, $F(3, 36)=6.995$; wild-type+RGS14 versus BDNF+/− +RGS14, Tukey's post hoc test, $P = 0.0061$). In contrast to mice subjected to $RGS14_{414}$ gene treatment, wildtype mice that were untreated or treated with vehicle exhibited no effect on ORM. The complete loss of RGS-mediated neuronal arborization and ORM enhancement after either deletion of BDNF or knockdown of 14-3-3ζ suggests that $RGS14_{414}$ exerts its function primarily through regulation of 14-3-3ζ-BDNF pathway activity. Moreover, considering that the memory enhancer effect of $RGS14_{414}$ was first observed at 20 days after treatment (Fig. 1*B*) and the structural plasticity, which is crucial for the memory enhancer effect of $RGS14_{414}$, occurred within 20 days of $RGS14_{414}$ treatment (Fig. 2*D–F*), we next examined whether 14-3-3ζ and BDNF levels in RGS-PRh animals 20 and 60 days after treatment correlate with the time frame of structural plasticity. We found that 14-3-3ζ levels in RGS-PRh animals 20 days after treatment were 112.01±3.71% higher (Fig. 4*E*; two-way ANOVA, $F(1, 6)=566.6$; vehicle versus RGS14, Sidak's post hoc test, $P<0.0001$) and BDNF levels were 71.67±3.71% higher (Fig. 4*E*; two-way ANOVA, $F(1, 10)=180.3$; vehicle versus RGS14, Sidak's post hoc test, $P<0.0001$), whereas 60 days after treatment, 14-3-3ζ levels were 19.02±1.38% ($P=0.0055$) higher and BDNF levels were 12.75±1.76% ($P=0.0024$) higher. These findings indicate that in RGS-PRh rats, there was very high activity in 14-3-3ζ-BDNF pathway within the period of structural plasticity (20 days). However, in contrast, a low level of activity was observed in 14-3-3ζ-BDNF pathway after 60 days of $RGS14_{414}$ treatment and this low activity in 14-3-3ζ-BDNF pathway coincided well with the period of inactivity in structural plasticity. Nevertheless, despite lower level of 14-3-3ζ and BDNF proteins in RGS-PRh rats after 60 days compared with that after 20 days of the treatment, both proteins remained significantly higher than vehicle-treated control animals ($P<0.0055$). These results suggest that there is a high correlation between 14-3-3ζ and BDNF levels and structural plasticity in RGS-PRh animals.

Prevention of Recognition and Spatial and Temporal Memory in Aging Rats

Our results demonstrate that $RGS14_{414}$ mediates its activity through the 14-3-3ζ-BDNF pathway and that activation of this pathway induces a robust increase in structural

plasticity and causes long-lasting memory enhancer capacity. Considering this permanent change in neuronal structure that is expected to reinforce synaptic connections and facilitate memory enhancement, we next questioned whether $RGS14_{414}$ gene treatment in the PRh could prevent memory deficits observed during normal aging and in Alzheimer's disease, the two most representative conditions in which deficits in memory have consistently been reported (Walsh and Selkoe 2004; Robitsek et al. 2008). In patients or individuals who display symptoms of memory deficit due to multiple etiologies, recognition, spatial, and temporal memory are principally affected (Brickman and Stern 2009). Therefore, we used normal aging Wistar rats and a transgenic *hAPPSwInd* mouse model of Alzheimer's disease (AD mice) to evaluate the effect of $RGS14_{414}$ gene treatment on the prevention of these types of memory. The studies were first performed in aging rats. We found that untreated rats of 6 and 12 months of age were able to retain information about an object in memory; however, when these rats reached 18months of age, a noticeable decrease in ORM was observed, with recognition memory falling to a level at which the rats were unable to recall the same information (Fig. 5*A*; one-way ANOVA, $F(3, 34)=32.76$; untreated 6 or 12 months versus untreated 18 months, Tukey's post hoc test, $P<0.0001$).However, treatment of rats with the $RGS14_{414}$ gene at 12 months of age prevented this deficit in ORM seen in untreated rats of 18 months of age, and this memory level was maintained even after 24 months of age (Fig. 5*A*; two-way ANOVA, $F(1, 20)=108.4$; vehicle versus RGS14 at 18 and 24 months, Sidak's post hoc test, $P<0.0001$). The performance of RGS-PRh rats at 18 and 24months of age reached a level similar to that of 6-monthold untreated animals. In contrast, vehicle treatment did not induce any effect on recognition memory, and the ORM levels of vehicle-treated rats were similar to those of untreated aged rats of 18 and 24 months of age.

To evaluate the effect of treatment on spatial memory, we performed behavioral studies using the Morris water maze (MWM) test. After 4 days of training, untreated rats of 18 months of age required much more time than untreated rats of 6 and 12 months of age to find the hidden platform in the MWM (Fig. 5*B*; one-way ANOVA, $F(3, 33)=17.01$; untreated 6 or 12 months versus untreated 18 months, Tukey's post hoc test, $P<0.0007$). However, when rats of 12 months of age were treated with the $RGS14_{414}$ gene in the PRh, their time to reach the hidden platform in the test performed at 18 months of age was noticeably reduced (Fig. 5*B*; two-way ANOVA, $F(1, 32)=31.55$; vehicle versus RGS14, Sidak's post hoc test, $P=0.0003$) (Supplementary Fig. 5*A*), and their performance was similar to that of untreated rats of 6 and 12 months of age. Furthermore, spatial memory in these RGS-PRh rats was maintained at the same level even at the age of 24 months (Fig. 5*B*; two-way ANOVA, $F(1, 32)=31.55$; vehicle versus RGS14, Sidak's post hoc test, $P=0.0022$). In contrast, treatment with vehicle exerted no effect on the performance of the rats. Thus, our results indicate that $RGS14_{414}$ treatment led to the prevention of spatial memory deficit seen in untreated rats of 18 and 24 months of age and that these aged RGS14-treated animals were able to retain information in the brain related to cues that guided the rats to locate the platform more efficiently than their untreated and vehicle-treated counterparts. The superior performance of RGS-PRh rats of 18 months of age was not due to a difference in swimming speed (Supplementary Fig. 5*B*), but it was

because of improved memory in retaining spatial information on the location of platform after 24 h (Supplementary Fig. 5*C*).

To test the effect of $RGS14_{414}$ treatment on the prevention of temporal memory in aging rats, the conditioned taste aversion (CTA) paradigm was used. Water-deprived rats were exposed to saccharine solution for 10min at night for two consecutive days. Saccharine solution was given in the morning on day 3, and immediately after drinking the solution, the rats were injected intraperitoneally with 0.1 M LiCl solution to evoke conditioning to saccharine intake at this time of day. From day 2 to day 6 after conditioning, these animals were given saccharine solution at night. On day 7 (test day), the animals were exposed to saccharine solution in the morning to test whether they were able to retain information related to the conditioning performed in the morning after saccharine intake. We considered that the animals that drank a significantly reduced volume of saccharine solution remembered the morning conditioning and that rats that drank more solution than during the previous session did not retain this information. We found that aged untreated rats of 18 months of age consumed considerably higher volumes of saccharine solution than untreated rats of 6 and 12 months of age (Fig. 5*C*; one-way ANOVA, $F(3, 28)=8.05$; untreated 6 or 12 months versus untreated 18 months, Tukey's post hoc test, $P<0.003$). These results suggest that untreated animals of 6 and 12 months of age could retain the information associated with morning saccharine intake conditioning and that aged untreated rats of 18 months of age were unable to retain this information. However, when rats of 12 months of age were treated with the $RGS14_{414}$ gene in the PRh, they were able to retain the same information in their memory in a test at 18 months of age; accordingly, reduced saccharine consumption by these aged RGS-treated animals was observed (Fig. 5*C*; two-way ANOVA, $F(1, 14)=45.28$; vehicle versus RGS14, Sidak's post hoc test, $P=0.0044$) (Supplementary Fig. 6). Additionally, the prevention of temporal memory deficits in these RGS-PRh rats was maintained at the same level even after 24 months of age (Fig. 5*C*; two-way ANOVA, $F(1, 14)=45.28$; vehicle versus RGS14, Sidak's post hoc test, $P=0.0045$). However, this RGS14-mediated prevention of temporal memory deficit in aging rats of 18 and 24 months of age was not observed when the rats were treated with vehicle.

Prevention of Recognition and Spatial and Temporal Memory in AD Mice

As described for aging rats, the ORM test was used to evaluate recognition memory, the MWM test was used to evaluate spatial memory, and the CTA paradigm was used to evaluate temporal memory in AD mice. In the ORM test, AD mice showed a noticeable ORM deficit at the age of 5 months (Fig. 6*A*; one-way ANOVA, $F(3, 40)=13.62$; 2.5months AD versus 5 months AD, Tukey's post hoc test, $P<0.0001$). Treatment of AD mice with the $RGS14_{414}$ gene in the PRh at the age of 2.5 months prevented the recognition memory deficits observed in AD animals at 5 months of age (Fig. 6*A*; two-way ANOVA, $F(1, 21)=95$; 5months;AD+vehicle versus AD+RGS14, Sidak's post hoc test, $P<0.0001$). RGS14-treated AD mice showed ORM levels similar to those of wild-type mice, and memory was maintained in these RGS-PRh animals even at the age of 7.5 months (Fig. 6*A*; two-way ANOVA, $F(1, 21)=95$; AD+vehicle versus AD+RGS14, Sidak's post hoc test, $P<0.0001$) and 10 months ($P=0.0005$). However, vehicle treatment

showed no effect on recognition memory, and the ORM levels of vehicle-treated mice were similar to those of untreated AD mice.

In the MWM test, we found that AD mice at 5 months of age required more time to reach the platform than AD mice at 2.5 months of age on day 4 of training (Fig. 6*B*; one-way ANOVA, $F(3, 36)=6.04$; 2.5 months AD versus 5 months AD, Tukey's post hoc test, $P=0.009$). However, when AD mice were treated with the $RGS14_{414}$ gene in the PRh at 2.5 months of age, their performance did not decrease, as was observed for AD animals at 5 months of age (Fig. 6*B*; two-way ANOVA, $F(1, 18)=35$; AD+vehicle versus AD+RGS14, Sidak's post hoc test, $P=0.0011$) (Supplementary Fig. 7*A*). The overall performance of RGS14-treated AD mice was similar to that of wild-type mice. In addition, the memory levels of these RGS-PRh AD mice were maintained after 7.5 months (Fig. 6*B*; two-way ANOVA, $F(1, 18)=35$; AD+vehicle versus AD+RGS14, Sidak's post hoc test, $P=0.0019$) and 10 months ($P=0.0063$) of age. In contrast, AD mice treated with vehicle showed a decrease in performance at 5 months of age, similar to untreated AD mice. These results indicate that $RGS14_{414}$ treatment in AD mice led to the prevention of spatial memory deficits similar to those in aged rats. The superior performance of $RGS14_{414}$-treated AD mice of 5 months of age was not due to a difference in swimming speed (Supplementary Fig. 7*B*), but itwas because of improved memory in retaining spatial information on the location of platform after 24 h of training (Supplementary Fig. 7*C*).

Morning conditioning to saccharine intake was evaluated in a manner similar to that described for the aged rat experiments. On the day of the test, the AD mice of 2.5 months of age were exposed to saccharine solution in the morning, and when aversion conditioning was invoked, the mice consumed less solution. However, AD mice of 5 months of age showed no aversive response to saccharine solution exposure (Fig. 6*C*; one-way ANOVA, $F(3, 32)=7.955$; 2.5 months AD versus 5 months AD, Tukey's post hoc test, $P=0.0021$). These data suggest that AD mice were unable to retain information in their memory associated with the morning conditioning to saccharine solution intake. Treatment of AD mice with $RGS14_{414}$ at the age of 2.5 months prevented this deficit in temporal memory in a test performed at 5 months of age, as these RGS-PRh AD mice consumed markedly less saccharine solution (Fig. 6*C*; two-way ANOVA, $F(1, 16)=69.56$; 5 months; AD+vehicle versus AD+RGS14, Sidak's post hoc test, $P=0.0002$), and their temporal memory level was similar to that of wild-type mice. We further observed that their intact memory at 5 months of age was maintained at the same level as in the RGS-PRh AD mice after 7.5 months (Fig. 6*B*; two-way ANOVA, $F(1, 16)=69.56$; AD+vehicle versus AD+RGS14, Sidak's post hoc test, $P=0.0004$) and 10 months of age ($P=0.0004$). Nevertheless, this prevention of temporal memory was not observed when AD mice were treated with vehicle.

Discussion

Our findings show that $RGS14_{414}$ gene treatment-mediated activation of 14-3-3ζ induces long-lasting memory-enhancing capacity in rats and causes structural plasticity that leads to more than two-fold increase in new dendritic spines in pyramidal neurons, which are

structures that innervate other brain regions and that primarily carry efferent synapses for synaptic communications between brain areas (Spruston 2008). An increase in dendritic spines of such scale is expected to cause synaptic reorganization in PRh neuronal circuit networks. The PRh is one of the main memory hubs, where various kinds of memory are converged (Masmudi-Martín et al. 2019), and the modulation of circuits of this brain area could result in a considerable effect on these types of memory. Therefore, an increase in PRh neuronal circuitry caused by the incorporation of new spines could promote more efficient memory-related information processing and facilitate memory formation in RGS-PRh animals. It has been shown that memory formation is critically associated with synaptic remodeling, including an increase in synapse number (Lamprecht and LeDoux 2004; Bailey et al. 2015). Memory is thought to be processed through interconnected brain circuits that are formed by the participation of distinct brain areas, and memory deficits occur as a consequence of reduced activity within these circuits (Hof and Morrison 2004; Dickerson and Eichenbaum 2010; Samson and Barnes 2013). Consistent with this observation, poor performance in patients with memory deficiency has been shown to be associated with decreased functional activity in medial temporal lobe neural networks (Daselaar et al. 2003; Dickerson and Eichenbaum 2010). Therefore, a permanent structural change through dendritic arborization in the PRh could promote memory enhancement by uplifting activity in the interconnected networks of the PRh. A sustained activity in these circuits could thus explain the long-lasting ORM-enhancing capacity in animals.

The $RGS14_{414}$ gene treatment-mediated increase in dendritic arborization and enhancement of ORM were dependent on 14- 3-3ζ-mediated BDNF signaling because either the knockdown of 14-3-3ζ or the deletion of BDNF ablated both of these effects. It has been shown that 14-3-3ζ protein forms a complex with receptor for activated C kinase 1 (RACK1) and is then transported to the nucleus, where it binds to exon IV of BDNF and promotes the transcription of the BDNF gene (Neasta et al. 2012). Thus, 14-3-3ζ regulates the transcription of the BDNF gene in a manner that is different from the CREB-BDNF pathway, which is susceptible to the activation of Ras/ERK1/2 (Sweatt 2004), cAMP/PKA (Wang and Storm 2003), and CaM kinase (Wayman et al. 2008) intracellular signaling, and the specific contribution of the 14-3-3ζ-BDNF pathway to BDNF-assigned biological functions has not been described. BDNF has been shown to play crucial roles in structural plasticity, neuronal branching, and the formation of synaptic connections, and it is essential for learning and memory (Waterhouse and Xu 2009; Lu et al. 2013; Kowian´ ski et al. 2018). Our findings indicate that the activation of 14-3-3ζ specifically induces BDNF-mediated structural plasticity and synaptic reorganization, which, in turn, facilitates memory formation in the brain. The direct relationship of 14-3-3ζ-mediated BDNF signaling with synaptic remodeling and memory-enhancing capacity suggests that this pathway might be involved in the maintenance of synaptic vigor and the sustenance of memory functions. Furthermore, reduced expression of the 14-3-3ζ gene, as observed in aging and Alzheimer's disease (Miller et al. 2008), can increase the vulnerability of these neuronal networks to deterioration. Consistent with this concept, mRNA and protein levels of BDNF were also decreased in aging and Alzheimer's disease (Narisawa-Saito et al. 1996; Connor et al. 1997; Hock et al. 2000; Michalski and Fahnestock 2003; Peng

et al. 2005). The upregulation of 14-3-3ζ through the treatment of $RGS14_{414}$ gene could prevent the decline in 14-3-3ζ-mediated BDNF signaling during aging and in Alzheimer's disease.

Since ORM enhancement was first detected 20 days after the treatment, we believe that an increase in the activity of 14-3-3ζ - mediated BDNF signaling initially induced dendritic arborization and the generation of new spines, which then enforced the reorganization of neuronal circuit connectivity in the PRh. This improved circuitry could have served as a structural substrate for the memory-enhancing effect of $RGS14_{414}$. The circuit reorganization occurred within 20 days of the treatment because further dendritic arborization was undetectable beyond this period, and this was the period when high activity in the 14-3-3ζ-BDNF pathway was observed. In addition, low activity in the 14-3-3ζ - BDNF pathway after 60 days of treatment coincided well with the inactivity in neuronal arborization. Therefore, the memory enhancing effect appears to emerge when novel connections are established and neural circuits are reorganized. Our results indicate that high 14-3-3ζ-BDNF pathway activity is essential for structural plasticity. However, low level of 14-3-3ζ-BDNF pathway activity observed 60 days after $RGS14_{414}$ treatment, which remains significantly higher than control animals, seems to be essential for the prevention of memory deficits. A low but sustained activity in the 14-3-3ζ-BDNF pathway might have arrested the awaited deterioration of the PRh neuronal networks and prevented the memory deficits in rodent models of aging and Alzheimer's disease.

The $RGS14_{414}$-mediated increase in 14-3-3ζ-BDNF pathway activity could facilitate exon IV-mediated BDNF transcription and augment BDNF levels, as observed in RGS-PRh animals. BDNF and its receptor TrkB are crucial for neuronal plasticity (Harward et al. 2016) and dendrite development (Wang et al. 2015), and autocrine BDNF–TrkB signaling inactivity reduces spine and dendrite growth. Thus, we propose that the initial increase in BDNF levels through 14-3-3ζ activation could amplify its effect through autocrine activity in the BDNF–TrkB pathway, which is linked to several important signaling pathways, including PLCγ -IP3-DAG, MEK1/2-ERK1/2, and AKT–mTOR. Therefore, the autocrine action of BDNF could amplify the initial effect through the activation of multiple signaling pathways. In contrast to CREB-BDNF pathway that requires external stimulus for its activation, the availability of 14-3-3ζ , as observed in RGS-PRh animals, might perpetuate this autocrine activity of BDNF without an external stimulus. Therefore, the prevention of memory deficits after $RGS14_{414}$ gene treatment in rodent models of aging and Alzheimer's disease was likely due to the preservation of 14-3-3ζ-BDNF pathway activity through perpetual BDNF autocrine activity. It seems that 14-3-3ζ-BDNF pathway is as an internal mechanism for consistent BDNF supply required for the maintenance of synaptic structures and related neuronal networks in brain, and a lower activity in this pathway could lead to the deterioration in these structures. An intact synaptic structures and related neuronal networks are crucial for adequate execution of memory functions.

On the other hand, upregulation of BDNF–TrkB signaling activity induces enhanced transmission at excitatory synapses (Poo 2001; Lu 2003) and this increase in excitatory synaptic transmission is mediated through both the presynaptic and the postsynaptic mechanisms (Minichiello 2009; Waterhouse and Xu 2009). On presynaptic side, BDNF

enhances glutamate release and increases the frequency of miniature excitatory postsynaptic currents (mEPSC) (Takei et al. 1998; Minichiello 2009). However, on the postsynaptic side, BDNF increases N-methyl-D-aspartate (NMDA) single-channel open probability through tyrosine phosphorylation of the NMDA receptor subunits NR1 and NR2B (Suen et al. 1997; Levine et al. 1998), modifies glutamatergic receptors (Caldeira, Melo, Pereira, Carvalho, Carvalho, et al. 2007b), and regulates the abundance of plasma membrane–bound glutamate receptors (Carvalho et al. 2008; Fortin et al. 2012). BDNF triggers phosphorylation of NR1 and NR2B subunits of NMDA receptor (Caldeira, Melo, Pereira, Carvalho, Carvalho, et al. 2007b) and upregulates the GluR1 and GluR2/3 subunits of α-amino-3-hydroxy-5-methyl-4-isoxazolepropionic acid (AMPA) receptors (Caldeira,Melo, Pereira, Carvalho, Correia, et al. 2007a; Fortin et al. 2012). In addition, BDNF also regulates the expression of NMDA receptor subunits by transcription-dependent mechanisms (Caldeira, Melo, Pereira, Carvalho, Carvalho, et al. 2007b; Carvalho et al. 2008). These modifications enhance the synaptic strength and initiate long-term potentiation (LTP), a process thought to constitute cellular substrates of learning and memory, in a Ca2+ concentration-dependent manner (Kang et al. 1997; Minichiello et al. 1999; Messaoudi et al. 2002). Furthermore, BDNF-dependent increase in the number of AMPA receptors at the postsynaptic membrane has been shown to enhance LTP (Derkach et al. 2007; Fortin et al. 2012). BDNF is also crucial for the long-term maintenance of AMPA receptor subunits and associated scaffolding proteins at synapses during long-term encoding of memory information (Jourdi et al. 2003). In summary, our work suggests that $RGS14_{414}$-mediated activation of 14-3-3ζ-BDNF pathway not only is adequate for preventing the types of memory that are particularly affected in patients with memory deficits but also is useful as a memory enhancer for long-term effects on memory.

Funding

Ministerio de Economía y Competitividad (BFU2013-43458-R); Junta de Andalucía (P12-CTS-1694, PI-0542-2013 to Z.U.K.).

Notes

Conflict of Interest: None declared.

References

Aitken A. 2006. 14-3-3 proteins: a historic overview. *Semin Cancer Biol*. 16:162–172.

Bailey CH, Kandel ER, Harris KM. 2015. Structural components of synaptic plasticity and memory consolidation. *Cold Spring Harb Perspect Biol*. 7:a021758.

Brennan GP, Jimenez-Mateos EM, McKiernan RC, Engel T, Tzivion G, Henshall DC. 2013. Transgenic overexpression of 14-3-3 zeta protects hippocampus against endoplasmic reticulum stress and status epilepticus in vivo. *PLoS One*. 8:e54491.

Brickman AM, Stern Y. 2009. Aging and memory in humans. *Encyclopedia Neurosci*. 1:175–180.
Broadie K, Rushton E, Skoulakis EM, Davis RL. 1997. Leonardo, a Drosophila 14-3-3 protein involved in learning, regulates presynaptic function. *Neuron*. 19:391–402.
Brown MW, Aggleton JP. 2001. Recognition memory: what are the roles of the perirhinal cortex and hippocampus? *Nat Rev Neurosci*. 2:51–61.
Caldeira MV, Melo CV, Pereira DB, Carvalho R, Correia SS, Backos DS, Carvalho AL, Esteban JA, Duarte CB. 2007a. Brain-derived neurotrophic factor regulates the expression and synaptic delivery of alpha-amino-3-hydroxy-5-methyl-4-isoxazole propionic acid receptor subunits in hippocampal neurons. *J Biol Chem*. 282:12619–12628.
Caldeira MV, Melo CV, Pereira DB, Carvalho RF, Carvalho AL, Duarte CB. 2007b. BDNF regulates the expression and traffic ofNMDA receptors in cultured hippocampal neurons. *Mol Cell Neurosci*. 35:208–219.
Carvalho AL,Caldeira MV, Santos SD,Duarte CB. 2008. Role of the brain-derived neurotrophic factor at glutamatergic synapses. *Br J Pharmacol*. 153(Suppl 1):S310–S324.
Cheah PS, Ramshaw HS, Thomas PQ, Toyo-Oka K, Xu X, Martin S, Coyle P, Guthridge MA, Stomski F, van den Buuse M, et al. 2012. Neurodevelopmental and neuropsychiatric behaviour defects arise from 14-3-3ζ deficiency. *Mol Psychiatry*. 17:451–466.
Chin J, Palop JJ, Puoliväli J, Massaro C, Bien-Ly N, Gerstein H, Scearce-Levie K, Masliah E, Mucke L. 2005. Fyn kinase induces synaptic and cognitive impairments in a transgenic mouse model of Alzheimer's disease. *J Neurosci*. 25:9694–9703.
Connor B, Young D, Yan Q, Faull RL, Synek B, Dragunow M. 1997. Brain-derived neurotrophic factor is reduced in Alzheimer's disease. *Brain Res Mol Brain Res*. 49:71–81.
Cornell B, Toyo-Oka K. 2017. 14-3-3 proteins in brain development: neurogenesis, neuronal migration and neuromorphogenesis. *Front Mol Neurosci*. 10:318.
Daselaar SM, Veltman DJ, Rombouts SA, Raaijmakers JG, Jonker C. 2003. Deep processing activates the medial temporal lobe in young but not in old adults. *Neurobiol Aging*. 24:1005–1011.
Derkach VA, Oh MC, Guire ES, Soderling TR. 2007. Regulatory mechanisms of AMPA receptors in synaptic plasticity. *Nat Rev Neurosci*. 8:101–113.
Dickerson BC, Eichenbaum H. 2010. The episodic memory system: neurocircuitry and disorders. *Neuropsychopharmacology*. 35:86–104.
Ennaceur A, Delacour J. 1988. A new one-trial test for neurobiological studies of memory in rats. 1: behavioral data. *Behav Brain Res*. 31:47–59.
Ernfors P, Lee KF, Jaenisch R. 1994. Mice lacking brain-derived neurotrophic factor develop with sensory deficits. *Nature*.368:147–150.
Escribano L, Simón AM, Pérez-Mediavilla A, Salazar-Colocho P, Del Río J, Frechilla D. 2009. Rosiglitazone reverses memory decline and hippocampal glucocorticoid receptor downregulation in an Alzheimer's disease mouse model. *Biochem Biophys Res Commun*. 379:406–410.

Fan X, Cui L, Zeng Y, Song W, Gaur U, Yang M. 2019. 14-3-3 proteins are on the crossroads of cancer, aging, and age-related neurodegenerative disease. *Int J Mol Sci*. 20:3518.

Fortin DA, Srivastava T, Dwarakanath D, Pierre P, Nygaard S, Derkach VA, Soderling TR. 2012. Brain-derived neurotrophic factor activation of CaM-kinase kinase via transient receptor potential canonical channels induces the translation and synaptic incorporation of GluA1-containing calciumpermeable AMPA receptors. *J Neurosci*. 32:8127–8137.

Gan Y, Ye F, He XX. 2020. The role of YWHAZ in cancer: a maze of opportunities and challenges. *J Cancer*. 11:2252–2264. *J Cancer*. 11:2252–2264.

Harward SC, Hedrick NG, Hall CE, Parra-Bueno P, Milner TA, Pan E, Laviv T, Hempstead BL, Yasuda R, McNamara JO. 2016. Autocrine BDNF-TrkB signalling within a single dendritic spine. *Nature*. 538:99–103.

Hock CH, Heese K, Olivieri G, Hulette CH, Rosenberg C, Nitsch RM, Otten U. 2000. Alterations in neurotrophins and neurotrophin receptors in Alzheimer's disease. *J Neural Transm Suppl*. 59:171–174.

Hof PR, Morrison JH. 2004. The aging brain: morphomolecular senescence of cortical circuits. *Trends Neurosci*. 27:607–613.

Jourdi H, Iwakura Y, Narisawa-Saito M, Ibaraki K, Xiong H, Watanabe M, Hayashi Y, Takei N, Nawa H. 2003. Brainderived neurotrophic factor signal enhances and maintains the expression of AMPA receptor-associated PDZ proteins in developing cortical neurons. *Dev Biol*. 263:216–230.

Kang H, Welcher AA, Shelton D, Schuman EM. 1997. Neurotrophins and time: different roles for TrkB signaling in hippocampal long-term potentiation. *Neuron*. 19:653–664.

Khan ZU, Fernando LP, Escribá P, Busquets X, Mallet J, Miralles CP, Filla M, De Blas AL. 1993. Antibodies to the human gamma 2 subunit of the gamma-aminobutyric acidA/benzodiazepine receptor. *J Neurochem*. 60:961–971.

Kowian´ ski P, Lietzau G, Czuba E, Was´kow M, Steliga A, Morys´ J. 2018. BDNF: a key factor with multipotent impact on brain signaling and synaptic plasticity. *Cell Mol Neurobiol*. 38:579–593.

Lamprecht R, LeDoux J. 2004. Structural plasticity and memory. *Nat Rev Neurosci*. 5:45–54.

Levine ES, Crozier RA, Black IB, Plummer MR. 1998. Brain-derived neurotrophic factor modulates hippocampal synaptic transmission by increasing *N*-methyl-d-aspartic acid receptor activity. *Proc Natl Acad Sci USA*. 95:10235–10239.

López-Aranda MF, López-Téllez JF, Navarro-Lobato I, Masmudi-Martín M, Gutiérrez A, Khan ZU. 2009. Role of layer 6 of V2 visual cortex in object-recognition memory. *Science*. 325:87–89.

Lu B. 2003. BDNF and activity-dependent synaptic modulation. *Learn Mem*. 10:86–98.

Lu B, Nagappan G, Guan X, Nathan PJ, Wren P. 2013. BDNFbased synaptic repair as a disease-modifying strategy for neurodegenerative diseases. *Nat Rev Neurosci*. 14:401–416.

Masmudi-Martín M, Navarro-Lobato I, López-Aranda MF, Delgado G, Martín-Montañez E, Quiros-Ortega ME, Carretero-Rey M, Narváez L, Garcia-Garrido MF, Posadas S, et al. 2019.
$RGS14_{414}$ treatment induces memory enhancement and rescues episodic memory deficits. *FASEB J*. 33:11804–11820.
McAllister AK, Katz LC, Lo DC. 1999. Neurotrophins and synaptic plasticity. *Annu Rev Neurosci*. 22:295–318.
Messaoudi E,Ying S-W,Kanhema T, Croll SD, Bramham CR. 2002. Brain-derived neurotrophic factor triggers transcriptiondependent, late phase long-term potentiation in vivo. *J Neurosci*. 22:7453–7461.
Michalski B, FahnestockM. 2003. Pro-brain-derived neurotrophic factor is decreased in parietal cortex in Alzheimer's disease. *Brain Res Mol Brain Res*. 111:148–154.
Miller JA, Oldham MC, Geschwind DH. 2008. A systems level analysis of transcriptional changes in Alzheimer's disease and normal aging. *J Neurosci*. 28:1410–1420.
Minichiello L. 2009.TrkB signalling pathways in LTP and learning. *Nat Rev Neurosci*. 10:850–860.
Minichiello L, Korte M, Wolfer D, Kühn R, Unsicker K, Cestari V, Rossi-Arnaud C, Lipp HP, Bonhoeffer T, Klein R. 1999. Essential role for TrkB receptors in hippocampus-mediated learning. *Neuron*. 24:401–414.
Morris R. 1984. Developments of a water-maze procedure for studying spatial learning in the rat. *J Neurosci Methods*. 11:47–60.
Morrison JH, Baxter MG. 2012. The ageing cortical synapse: hallmarks and implications for cognitive decline. *Nat Rev Neurosci*. 13:240–250.
Mucke L, Masliah E, Yu GQ, Mallory M, Rockenstein EM, Tatsuno G, Hu K, Kholodenko D, Johnson-Wood K, McConlogue L. 2000. High-level neuronal expression of abeta 1-42 in wildtype human amyloid protein precursor transgenic mice: synaptotoxicity without plaque formation. *J Neurosci*. 20: 4050–4058.
Murray EA, Richmond BJ. 2001. Role of perirhinal cortex in object perception, memory, and associations. *Curr Opin Neurobiol*. 11:188–193.
Narisawa-Saito M, Wakabayashi K, Tsuji S, Takahashi H, Nawa H. 1996. Regional specificity of alterations in NGF, BDNF and NT-3 levels in Alzheimer's disease. *Neuroreport*. 7:2925–2928.
Neasta J, Kiely PA, He DY, Adams DR, O'Connor R, Ron D. 2012. Direct interaction between scaffolding proteins RACK1 and 14-3-3ζ regulates brain-derived neurotrophic factor (BDNF) transcription. *J Biol Chem*. 287:322–336.
Palop JJ, Jones B, Kekonius L, Chin J, Yu GQ, Raber J, Masliah E, Mucke L. 2003. Neuronal depletion of calcium-dependent proteins in the dentate gyrus is tightly linked to Alzheimer's disease-related cognitive deficits. *Proc Natl Acad Sci USA*. 100:9572–9577.
Paxinos G,Watson C. 1998. *The rat brain in stereotaxic coordinates*. San Diego (CA): Academic Press. Paxinos G, Franklin KBJ. 2001. *The mouse brain in stereotaxic coordinates*. San Diego (CA): Academic Press.
Peng S,Wuu J, Mufson EJ, Fahnestock M. 2005. Precursor form of brain-derived neurotrophic factor and mature brain-derived neurotrophic factor are decreased in the pre-clinical stages of Alzheimer's disease. *J Neurochem*. 93:1412–1421.

Philip N, Acevedo SF, Skoulakis EM. 2001. Conditional rescue of olfactory learning and memory defects in mutants of the 14-3-3zeta gene leonardo. *J Neurosci*. 21:8417–8425.
Poo MM. 2001. Neurotrophins as synaptic modulators. *Nat Rev Neurosci*. 2:24–32.
Qiao H, Foote M, Graham K,Wu Y, Zhou Y. 2014. 14-3-3 proteins are required for hippocampal long-term potentiation and associative learning and memory. *J Neurosci*. 34:4801–4808.
Robitsek RJ, Fortin NJ, Koh MT, Gallagher M, Eichenbaum H. 2008. Cognitive aging: a common decline of episodic recollection and spatial memory in rats. *J Neurosci*. 28:8945–8954.
Sadik G, Tanaka T, Kato K, Yamamori H, Nessa BN, Morihara T, Takeda M. 2009a. Phosphorylation of tau at Ser214 mediates its interaction with 14-3-3 protein: implications for the mechanism of tau aggregation. *J Neurochem*. 108:33–43.
Sadik G, Tanaka T, Kato K, Yanagi K, Kudo T, Takeda M. 2009b. Differential interaction and aggregation of 3-repeat and 4- repeat tau isoforms with 14-3-3zeta protein. *Biochem Biophys Res Commun*. 383:37–41.
Samson RD, Barnes CA. 2013. Impact of aging brain circuits on cognition. *Eur J Neurosci*. 37:1903–1915.
Shimada T, Fournier AE, Yamagata K. 2013. Neuroprotective function of 14-3-3 proteins in neurodegeneration. *Biomed Res Int*. 2013:564534.
Skoulakis EM, Davis RL. 1996. Olfactory learning deficits in mutants for leonardo, a Drosophila gene encoding a 14-3-3 protein. *Neuron*. 17:931–944.
Skoulakis EM, Davis RL. 1998. 14-3-3 proteins in neuronal development and function. *Mol Neurobiol*. 16:269–284.
Spruston N. 2008. Pyramidal neurons: dendritic structure and synaptic integration. *Nat Rev Neurosci*. 9:206–221.
Suen PC, Wu K, Levine ES, Mount HT, Xu JL, Lin SY, Black IB. 1997. Brain-derived neurotrophic factor rapidly enhances phosphorylation of the postsynaptic *N*-methyl-d-aspartate receptor subunit 1. *Proc Natl Acad Sci USA*. 94:8191–8195.
Sweatt JD. 2004. Mitogen-activated protein kinases in synaptic plasticity and memory. *Curr Opin Neurobiol*. 14:311–317.
Takei N, Numakawa T, Kozaki S, Sakai N, Endo Y, Takahashi M, Hatanaka H. 1998. Brain-derived neurotrophic factor induces rapid and transient release of glutamate through the non-exocytotic pathway from cortical neurons. *J Biol Chem*. 273:27620–27624.
Toyo-oka K,Wachi T, Hunt RF, Baraban SC, Taya S, Ramshaw H, Kaibuchi K, Schwarz QP, Lopez AF, Wynshaw-Boris A. 2014. 14-3-3ε and ζ regulate neurogenesis and differentiation of neuronal progenitor cells in the developing brain. *J Neurosci*. 34:12168–12181.
Umahara T, Uchihara T, Iwamoto T. 2012. Structure-oriented review of 14-3-3 protein isoforms in geriatric neuroscience. *Geriatr Gerontol Int*. 12:586–599.
Walsh DM, Selkoe DJ. 2004. Deciphering the molecular basis of memory failure in Alzheimer's disease. *Neuron*. 44: 181–193.
Wang H, Storm DR. 2003. Calmodulin-regulated adenylyl cyclases: cross-talk and plasticity in the central nervous system. *Mol Pharmacol*. 63:463–468.

Wang L, Chang X, She L, Xu D, Huang W, Poo MM. 2015. Autocrine action of BDNF on dendrite development of adult-born hippocampal neurons. *J Neurosci*. 35:8384–8393.
Waterhouse EG, Xu B. 2009. New insights into the role of brain derived neurotrophic factor in synaptic plasticity. *Mol Cell Neurosci*. 42:81–89.
Wayman GA, Lee YS, Tokumitsu H, Silva AJ, Soderling TR, Soderling TR. 2008. Calmodulin-kinases: modulators of neuronal development and plasticity. *Neuron*. 59: 914–931.
Winters BD, Saksida LM, Bussey TJ. 2008. Object recognition memory: neurobiological mechanisms of encoding, consolidation and retrieval. *Neurosci Biobehav Rev*. 32:1055–1070.
Xu X, Jaehne EJ, Greenberg Z, McCarthy P, Saleh E, Parish CL, Camera D, Heng J, Haas M, Baune BT, et al. 2015. 14-3-3ζ deficien tmice in the BALB/c background display behavioural and anatomical defects associated with neurodevelopmental disorders. *Sci Rep*. 5:12434.

Figures

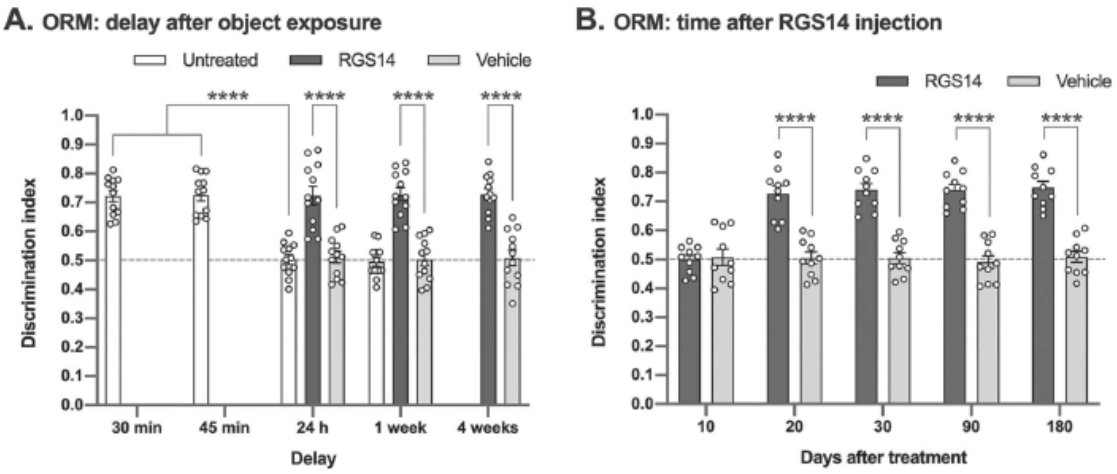

Figure 1. $RGS14_{414}$ gene treatment induces ORM enhancement and dendritic arborization. (*A*) After exposure to an object, 3-month-old normal untreated rats were able to retain object information in memory for 30 and 45 min; however, they were unable to retain such information after 24 h. $RGS14_{414}$ gene treatment of the PRh in these rats induced ORM enhancement that was observed at 24 h, 1 week, and 4 weeks, whereas vehicle treatment induced no effect. Dotted lines across panels *A* and *B* indicate the threshold at which (0.5 DI and below) the animals were unable to retain object information in memory. n=12 (unfilled circle). (*B*) Memory enhancement in rats appeared after 20 days after treatment with the RGS14414 gene, and this memory-enhancing effect persisted for a long time in these animals. n=10. **** (one-way ANOVA with Tukey's post hoc test in *A* and two-way ANOVA with Sidak's post hoc test in *A, B, P*<0.0001).

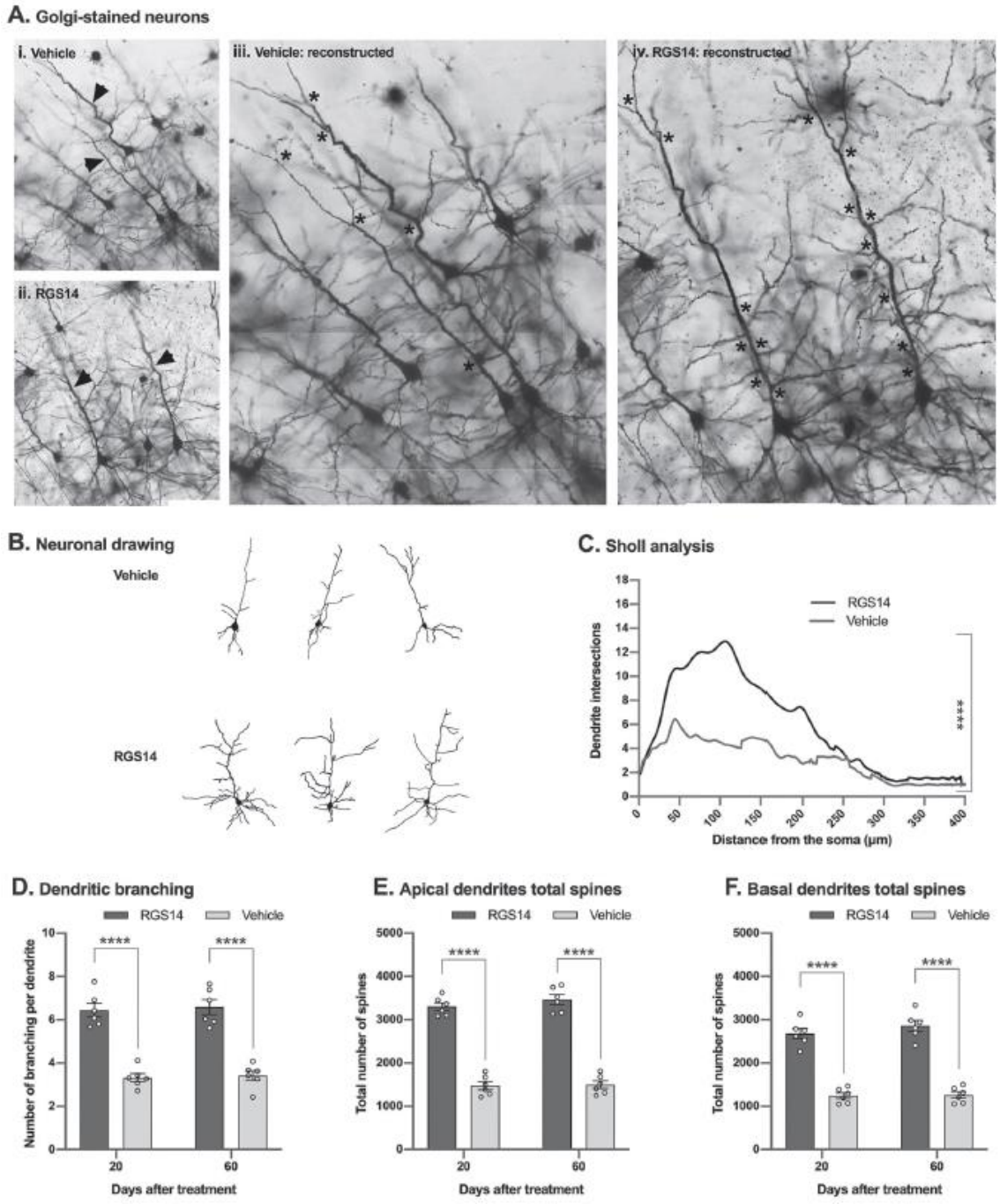

Figure 2. RGS14$_{414}$ gene treatment causes dendritic arborization. (*A*) Images of Golgi-stained neurons from vehicle- and RGS 14-treated rat brain sections. Images *i* and *ii* are single frame image acquired with single focus, and *iii* and *iv* are reconstructed from multifocus images of *i* and *ii*, respectively. Arrows in *i* and *ii* indicate two pyramidal neurons that were used as reference to acquire multifocus images for *i* and *ii* to do the frame reconstruction. Stars in reconstructed images iii and iv indicate the branching sites. (*B*) Neuronal drawings representing examples of pyramidal neurons from vehicle- and RGS14-treated rats. (*C*) Sholl analysis of pyramidal neurons showing increase in neuronal arborization in RGS14$_{414}$-treated animals. *n*=6 (*D*) RGS-treated animals showed a robust increase in the number of dendritic branches in pyramidal neurons after 20 and 60 days

of treatment with the RGS14$_{414}$ gene. *n*=6. (*E* and *F*) Coinciding with the increment in dendritic branching, an upsurge in total spine number of apical dendrites (*E*) and basal dendrites (*F*) was observed in RGS14-treated animals. *n*=6. ∗∗∗∗ (two-tailed unpaired *t* test in *C*; two-way ANOVA with Sidak's post hoc test in *D*, *E*, and *F*, *P*<0.0001).

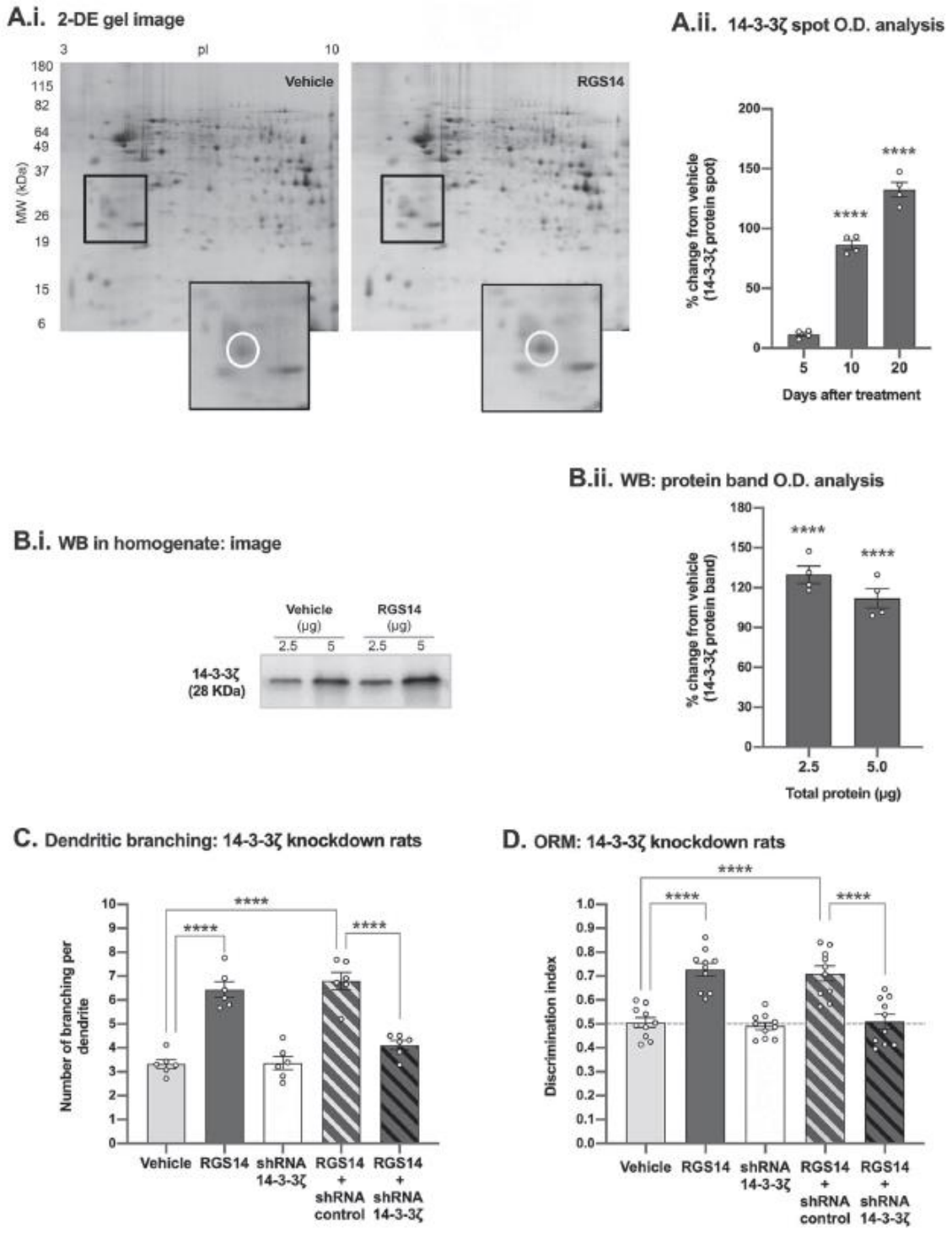

Figure 3. $RGS14_{414}$ mediates its effect through 14-3-3ζ . (*A.i*) 2-DE gels of proteomics display the protein spots corresponding to 14-3-3ζ protein (white circle) of vehicle and $RGS14_{414}$-treated rats 20 days after treatment. (*A.ii*) Optical density analysis of spots from 2-DE gels revealed a robust increase in 14-3-3ζ protein levels 5, 10, and 20 days after treatment. *n*=4 (unfilled circles; two experiments from each of the two sets of brain homogenates prepared from a pool of four rat brains each). (*B.i*) An example of western blots performed with 2.5 and 5 μg of brain homogenate protein exhibiting the expression of 14-3-3ζ protein 20 days after RGS14414 gene treatment. (*B.ii*) Analysis of optical density values of immunoreactive bands of 14-3-3ζ protein revealed a more than 2-fold increase in 14-3-3ζ protein levels in RGS14-treated animals. *n*=4 (two experiments from each of the two sets of brain homogenates prepared from a pool of four rat brains each). (*C*) An injection of 14-3-3ζ shRNA into the PRh completely abolished dendritic branching, which was observed after $RGS14_{414}$ gene treatment, in animals 20 days after treatment (*n*=6) and (*D*) further eliminated $RGS14_{414}$-mediated ORM enhancement. *n*=10. ∗∗∗∗ (two-way ANOVA with Sidak's post hoc test in *A.ii* and *B.ii*; one-way ANOVA with Tukey's post hoc test in *C* and *D*; $P < 0.0001$).

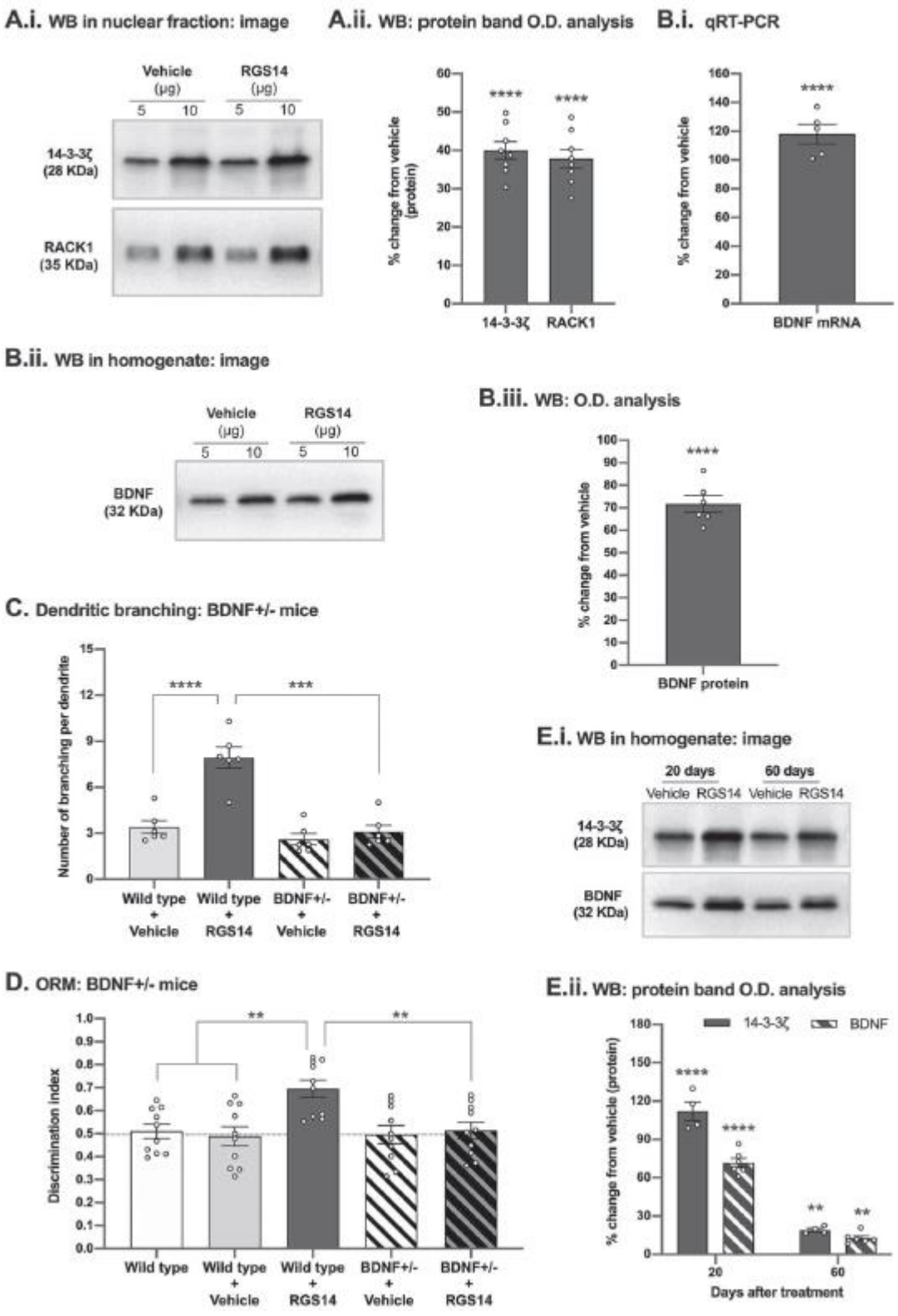

Figure 4. The 14-3-3ζ-BDNF pathway in RGS14$_{414}$–mediated structural plasticity and ORM enhancement. (*A.i*) An example western blot performed with 5 and 10 μg of nuclear fraction protein showing the expression of 14-3-3ζ and RACK1 proteins 20 days after RGS14$_{414}$ gene treatment, and (*A.ii*) optical density values of the immunoreactive bands of 14-3-3ζ and RACK1 proteins showing similar levels of increase in both proteins in the

nucleus. *n*=8 (unfilled circles; four experiments from each of the two sets of brain nuclear fractions prepared from a pool of four rat brains each). (*B.i*) qRT-PCR analysis shows that RGS14 gene treatment increased BDNF mRNA levels. *n*=5. (*B.ii*) An example western blot showing BDNF protein expression 20 days after RGS14 gene treatment, and (*B.iii*) an analysis of the optical density values of the western blot bands demonstrating an increase in BDNF protein levels similar to the increase in BDNF mRNA levels. *n*=6 (three experiments from each of the two sets of brain homogenates prepared from a pool of four rat brains each). (*C*) RGS14414 treatment in wild-type mice induced a robust increase in pyramidal dendritic branching; however, this effect disappeared when the same treatment was administered to BDNF-deficient (BDNF+/−) mice. *n*=6. (*D*)Wild-type mice displayed enhanced ORM after treatment with RGS14 (wild-type+RGS14), whereas this memory-enhancing effect of RGS14 was absent in BDNF+/− mice (BDNF+/− +RGS14). The dotted line across the figure indicates the threshold at which (0.5 DI and below) the animals were unable to retain object information in memory. *n*=10. (*E.i*) An example western blot showing 14-3-3ζ and BDNF proteins expression after 20 and 60 days of RGS14 gene treatment, and (*E.ii*) an optical density analysis of western blot bands revealed high increase in 14-3-3ζ and BDNF proteins 20 days after $RGS14_{414}$ gene treatment; however, after 60 days, the increase in both protein was lower than after 20 days. Nevertheless, this low-level increase after 60 days of treatment in both 14-3-3ζ and BDNF proteins remained significantly higher than vehicle-treated animals. *n*=4 (14-3-3ζ) and 6 (BDNF) (two and three experiments, respectively, from each of the two sets of brain homogenates prepared from a pool of four rat brains each). ∗∗ (one-way ANOVA with Tukey's post hoc test in *D*; two-way ANOVA with Sidak's post hoc test in *E.ii*, $P<0.01$), ∗∗∗ (one-way ANOVA with Tukey's post hoc test in *C*, $P=0.0001$), ∗∗∗∗ (two-way ANOVA with Sidak's post hoc test in *A.ii* and *E.ii*; two-tailed unpaired *t* test in *B.i* and *B.iii*; one-way ANOVA with Tukey's post hoc test in *C*; $P<0.0001$).

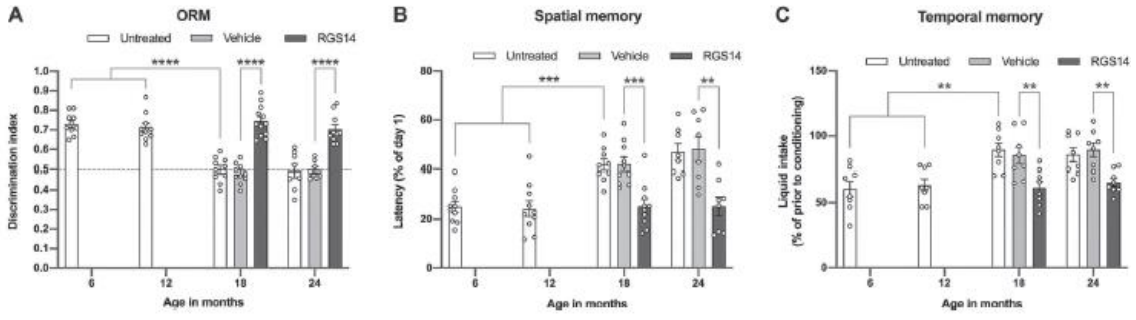

Figure 5. Prevention of recognition and spatial and temporal memory in aging rats. (*A*) In the recognition memory test, when untreated rats of 6 and 12 months of age were exposed to an object, they could retain the object information in memory; however, untreated rats of 18 months of age were unable to retain this information. $RGS14_{414}$ gene treatment delivered to the PRh of rats at 12 months of age prevented the recognition memory deficits seen at 18 months of age, and the memory of these $RGS14_{414}$-treated rats

was maintained even at 24 months of age. The dotted line across the figure indicates the threshold at which (0.5 DI and below) the animals were unable to retain object information in memory. n=10–12 (unfilled circle). (*B*) shows the results of the spatial memory test. Four days after learning the MWM, untreated rats of 6 and 12 months of age took considerably less time to find the platform; however, untreated rats of 18 months of age needed much more time to reach the platform, and their performance was significantly poorer. However, when rats of 12 months of age were treated with the $RGS14_{414}$ gene, the spatial memory deficiency that should have been observed at 18 months of age was prevented, and their performance was far superior to that of untreated and vehicle-treated animals. These rats showed spatial memory levels similar to those of 6-month-old untreated rats. These spatial memory levels in RGS14 animals remained at 24 months of age. n=10. (*C*) shows the results of the temporal memory test. In contrast to 18-month-old untreated rats that failed to remember the morning taste aversion conditioning, untreated rats of 6 and 12 months of age were able to retain this information in memory. Treatment of rats of 12 months of age with the $RGS14_{414}$ gene prevented the temporal memory deficit seen in rats of 18 months of age, and their response to morning taste conditioning was the same as the response of 6-month-old untreated animals. The level of temporal memory in RGS14-treated rats was preserved at 24 months of age. n=8. ∗∗ (one-way ANOVA with Tukey's post hoc test in C and two-way ANOVA with Sidak's post hoc test in *B* and *C*; $P<0.008$), ∗∗∗ (one-way ANOVA with Tukey's post hoc test in *B* and two-way ANOVA with Sidak's post hoc test in *B*, $P<0.0007$), ∗∗∗∗ (one-way ANOVA with Tukey's post hoc test in *A* and two-way ANOVA with Sidak's post hoc test in *A*, $P<0.0001$).

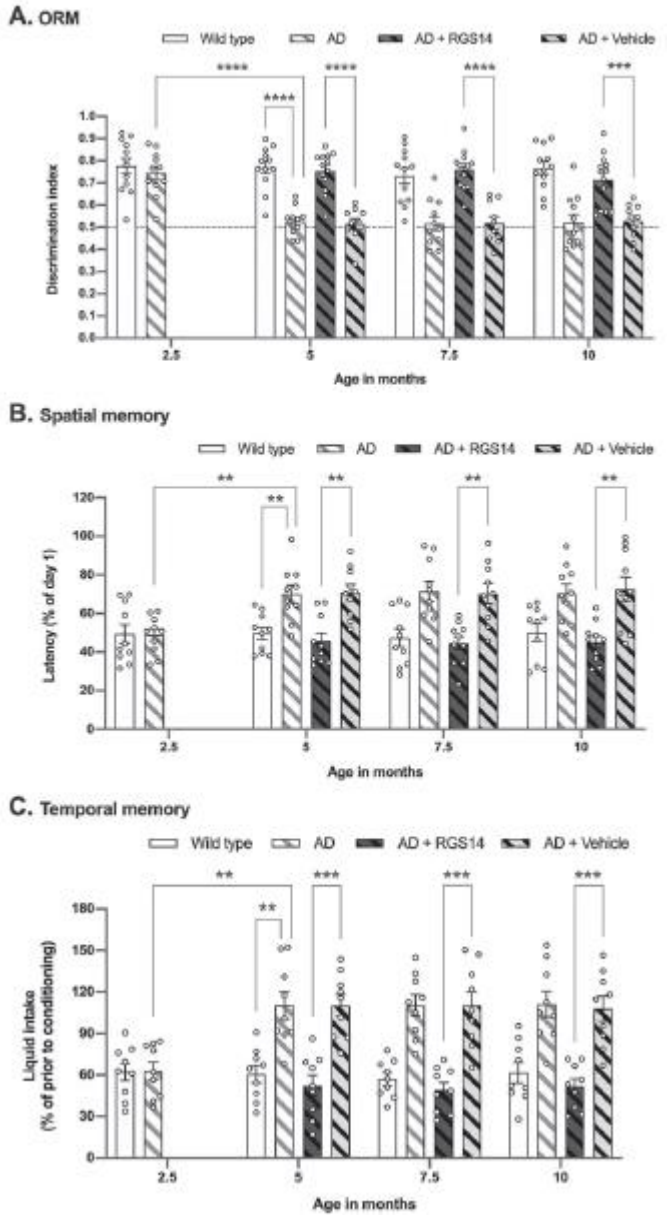

Figure 6. Prevention of recognition and spatial and temporal memory in AD mice. (*A*) In the object recognition memory test, AD mice showed substantial memory deficits at the age of 5 months compared with wild-type mice. $RGS14_{414}$ gene treatment in the PRh of AD mice at 2.5 months of age led to the prevention of recognition memory deficits observed at 5 months of age, and they showed recognition memory levels similar to those of wild-type mice. This level of memory was preserved through the age of 7.5 and 10 months. The dotted line across the figure indicates the threshold (0.5 DI and below) at which the animals were unable to retain object information in memory. n=10–13 (unfilled circle). (*B*) Spatial memory results in AD mice. AD mice at 5 months of age needed more time to reach the platform than wild-type mice, and their performance was noticeably worse. However, treatment with $RGS14_{414}$ in 2.5-month-old AD mice prevented the spatial memory deficit seen in AD mice at the age of 5 months. These AD+RGS14mice showed better performance in the MWM than wild-type mice, and this level of spatial memory was maintained through the age of 7.5 and 10 months. n=10. (*C*) Temporal

memory results in AD mice. AD mice of 5 months of age were unable to retain information from morning taste aversive conditioning, whereas wild-type mice could retain this information in memory. However, when AD mice of 2.5 months of age were treated with $RGS14_{414}$, the temporal memory deficit that should have been observed at 5months of age was prevented, and these mice consumed much less solution, similar to wild-type mice. This level of temporal memory was preserved through the age of 7.5 and 10 months. n=9. ∗∗ (one-way ANOVA with Tukey's post hoc test in *B* and two-way ANOVA with Sidak's post hoc test in *C*, P<0.009), ∗∗∗ (two-way ANOVA with Sidak's post hoc test in *A* and *C*, P<0.0004), ∗∗∗∗ (one-way ANOVA with Tukey's post hoc test and two-way ANOVA with Sidak's post hoc test in *A*, P<0.0001).